

We thank both reviewers for their detailed comments which helped us to substantially revise this paper. Here below is a summary of the main changes we made.

- the introduction was lengthy, not very clear due to technical wording and not focused on the subject of the paper, i.e. the impact of coupling with the ocean and the role of the surface fluxes. We removed some unnecessary details and added some information on the lack of clear medicane definition.
- the time evolution of the cyclone and its different phases are assessed in a more objective way, based on the low-level temperature field and upper-level PV anomaly. This leads to a slightly different timing of the event, but does not change the conclusions. Two figures seemed unnecessary and were removed, a figure showing the overall time evolution has been added, a figure comparing the rainfall rates during two phases has been added.
- the description of the different phases, in term of surface versus upper-level mechanisms has been shortened and merged with the analysis of the surface fluxes (Section 4). Only a short description of the cyclone chronology has been kept in Section 3.
- we provide more details on how our results (in terms of cyclone track or thermal winds) compare with other results on the same case.

We provide below detailed answers to the reviewers comments.

AR #1

Major points:

- The distinction among the three different phases in the cyclone lifetime is subjectively defined, thus not completely convincing. I recommend you find an objective way, e.g. based on the Hart (2003) diagram, or on the methodology discussed in Fita and Flaounas (2018).

Yes, this is an important comment, and we realized that the classification was probably not appropriate. The phase diagram, in this case, was not sufficient to distinguish between the different phases. We choose to use the upper level and low level dynamics (300 and 850 hPa) as in Fita and Flaounas (2018) (their Fig. 6) to investigate the cyclone evolution and separate the different phases in a more objective way. The description of the chronology of the medicane (section 3.1) is now based on a figure similar to the one of Fita and Flaounas (2018) and on the Hart (2003) diagram. The latter has been changed to make it similar to the one of Fita and Flaounas (2018) and to make the different phases easier to distinguish. The evolution of the medicane follows 3 phases, development, mature phase and decay, they are time shifted with respect to the previous classification. One figure has been added (Fig. 5), all the figures showing time series has been redone with colour codes corresponding to this new chronology, and the discussion about the evolution of the air-sea heat fluxes and the respective roles of the surface parameters has also been changed. The new time periods we consider (in Tables 1 to 3 and Figures 13, 16 and 18) are representative of these phases of the event. We feel that this chronology based on more objective criteria is more robust and that the corresponding analysis is easier to follow.

- The discussion in Section 3.1 is not convincing in many points (see also minor points in 3.1.1 and 3.1.2):

L280-285: the bands of colder air may not be due to the evaporation of precipitation. In particular, the one to the left may be due to cold-air advection, which secludes the cyclone warm core, turning around the center within the cyclonic circulation, as suggested by Fig. 6a. To clarify this aspect, one should perform numerical simulations without the evaporation of precipitation: this would demonstrate whether the cold air is due to a long-range transport toward the center of the cyclone or really to the evaporation of precipitation.

We understand your point, so numerical simulations without the cooling due to the evaporation of the precipitation were done, and the comparison of the virtual potential temperature at low level shows clearly that the bands of colder air are actually due to the rain evaporation (see Fig. R1 without cooling with respect to Fig. R2 with cooling).

We feel not necessary to add this figure in the manuscript, but we now mention the results of this additional run as an evidence of the origin of these cold pools, versus the cold air advected from the North African coasts, which are still present in the simulation without the cooling due to rain evaporation.

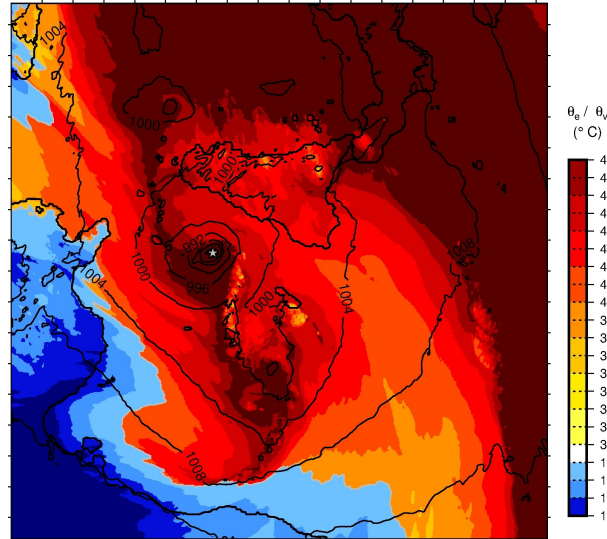


Figure R1: Map of equivalent potential temperature (warm colors) and virtual potential temperature below 19 °C (blue shades), and SLP (black contours) at 08:30 UTC on 7 November, when the cooling due to rain evaporation is turned off.

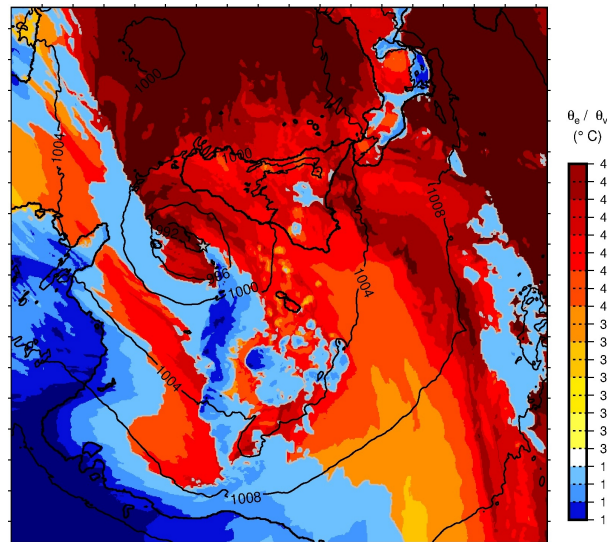


Figure R2: Map of equivalent potential temperature (warm colors) and virtual potential temperature below 19 °C (blue shades), and SLP (black contours) at 08:30 UTC on 7 November.

L286-288: I understand that your focus is on surface fields, but you should also consider what happens in the levels immediately above (e.g., 950 hPa, 900 hPa) to support your considerations and better identify the origin of the different air masses and thermal gradients. The vertical extension of the cold air masses in North African may be limited to a few meters, so you should demonstrate more clearly that the “advection of cold and dry air . . . from the Tunisian and Libyan continental surface . . . (L296-297, L448-449)” is relevant. For example, you can use backtrajectories, going earlier in time than those shown in Fig. 9, to clearly illustrate the origin of the air parcels.

We are not sure to understand this comment, as the vertical extension of the air masses both in the cold pools due to rain evaporation and those advected from North Africa is visible in the vertical cross section in (former) Fig. 7b. This figure has been reduced in the new version, as we think that two vertical cross sections were redundant to illustrate the role of cold pools. We keep the E-W section, that clearly shows, in consistency with (former) Fig. 7a, the extension of both the cold pools due to evaporation (between 500 and 1000 m) and of the cold air advected from North Africa (between 1000 and 1500 m).

Minor points:

Lines 9-12: “The deepening . . . of the cyclone is due . . . then to low-level convergence and uplift of conditionally unstable air masses by cold pools, resulting either from rain evaporation or from advection of continental air masses from North Africa.”: the deepening can be due to WISHE mechanism and/or to baroclinic processes, the way precipitation is generated is related to convergence and uplift by cold pools, so the sentence should be reformulated.

Yes, this has been reformulated, “Heavy precipitation result from uplift of conditionally unstable air masses due to low-level convergence at sea”

Line 14: . . . due to a sea surface cooling . . .

Yes, change done.

Line 27: at least up to the mid troposphere . . . : really, even in the version of Hart diagram modified by Picornell et al. (2014) you used, the vertical structure is analyzed also in the upper troposphere, up to 400 hPa.

Yes, we analysed the vertical structure up to 400 hPa, but there was a typo in the legend of Fig. 4. This has been corrected.

Line 33: note that the 26 ° C threshold of tropical cyclones cannot be applied to tropical cyclones developing from tropical transition processes (see McTaggart-Cowen et al., 2015).

Yes, we added the reference, and a short comment on that. Thank you.

Line 41, 274: I image you are referring to lee cyclones (see Tibaldi et al., 1990), not to lee waves. Lee cyclones are not only the effect of a wave, but theory provides a comprehensive way to describe the process of cyclogenesis.

This has been changed to “lee cyclones forming south of the Alps or north of the North African reliefs (Tibaldi et al., 1990)”, thank you for the reference.

Line 119: . . . its initiation as a baroclinic storm . . .

This sentence has been removed.

Section 2.1: I understand that 19 Figures are a lot, but please consider the possibility to include additional 1-2 figures to make easier to understand the results in this Section, or refer to Figures published in previous papers.

Yes, we realized that this part is not easy to follow. We added one figure (Fig. 1) showing the upper-level PV anomaly, SLP and temperature at 850 hPa from the ERA-5 outputs at two epochs to make the large-scale description of the chronology of the event easier to follow.

Line 144: please refer to Fig. 1 to help following the text.

Yes, we refer here to (now) Fig. 3.

Line 170: Is convection treated explicitly? Please add this piece of information.

Done “In this configuration, deep convection is explicitly represented while shallow convection is parametrized using the eddy diffusivity Kain-Fritsch scheme (Pergaud et al., 2009).”

Line 171: grid spacing instead of resolution.

Change done.

Line 189: what is an ORCA grid?

We added the piece of information “(tripolar grid with variable resolution, Madec and Imbart, 1996)”.

Section 2.2.3: what is the rationale behind the choice of this domain extension? Have you tried with different domains? Apparently, only a small domain extension is favorable for a proper simulation of the track - cfr. Cioni et al. (2018) and your tracks with those in Carriò et al. (2017) and Pytharoulis et al. (2018). Please, comment on this.

The only test we made was to use only one domain with a resolution of 2 km, boundary forcing and initial conditions from the ECWMF analyses, without grid nesting. The domain extension, however, was similar to the D2 extension used in this study. We obtained a better track, but no deepening of the cyclone. The present D2 domain has been chosen to cover the cyclone evolution, including the surrounding coasts. Possibly, a simulation with a smaller nested domain with finer resolution like in Cioni et al. (2018) would lead to a better simulated track, but we did not test this (also because we wanted our resolution to be comparable with the one of the operational AROME forecasts, 1.3 km). We added a comment on this “This domain extension was chosen as a trade-off between computing time and an extension large enough to represent the physical processes involved in the cyclone lifecycle, including the influence of the coasts”.

Figure 3a: it would be helpful to add at least the maximum wind recorded in Lampedusa, Malta, Pantelleria in panel a.

Yes, they were added.

L274: . . . by the lee cyclone induced by the North African relief . . .

Yes, change done.

L279-280: note that it is not the convergence between SE flow and S-SW flow responsible for the most intense precipitation at sea in Fig. 6b, but the one associated with the low-level southwesterlies and the northwesterly flow behind.

We were referring here to the convergence line east of the domain, at the cold front.

L284: northwestwards?

We are referring to the cold air advected from the African coasts, and the flow is actually northeastwards.

L285: deep convection in . . .

This paragraph has been removed.

L292: The low-level virtual . . .

Yes, change done.

L300: in the southeasterly low-level flow . . . (in Fig. 7b, the wind component seems from the south).

Part of the flow (in the SE of the cyclonic centre) is southeasterly and part of it (NW of the cyclonic centre) is northwesterly, that is why low-level convergence at sea is strong. We were referring here to the NW flow.

L302-305: did you check these points in the simulation? May you be more quantitative?

The dry air intrusion with the values of the RH were checked, they are visible Fig. 15, and we now refer to it. The other points were not, and we preferred to remove them.

L306: the high CAPE is not obtained by extracting heat and moisture! The surface fluxes modify the low-level features, determining an environment more favorable to instability (i.e., CAPE increased).

Yes. This paragraph has been removed, due to a major comment of Reviewer #2.

L316-318: again, this sentence should be less qualitative in order to be more convincing.

Actually, this sentence has been removed, as we feel it unnecessary after the more quantitative description based on Fig. 15. The role of latent heat release has been assessed using the backtrajectories and the separate evolution of potential temperature and humidity along the trajectories and this is detailed in sect. 4.4.

L323: Mazza et al. (2017) does not refer to the December 2005 Mediane.

Yes, thank you for checking, this has been corrected.

L331: you really show the role of air-sea interaction processes; the role of diabatic processes may be inferred from theory, you do not show that it occurs in this case.

This part has been changed, we added an assessment of the temperature and humidity evolution during the particle travel at sea first, then during its uplift. This shows more clearly that the latent heating is at play during the uplift of the particle.

L342-343: I suggest to change “the evolution of the SST” with “sea currents”.

Really, the object of section 3.2.1 (now 3.2) was to check the evolution of the SST in the coupled simulation and its impact on the atmosphere. The currents play a secondary role. As this part has been changed, the sentence now reads “In the following, the possible impact of the ocean–atmosphere coupling on the cyclone intensity is examined by comparing the results of the CPL, NOCUR, and NOCPL simulations. The time period for this comparison is the 7 November only, as the medicane has lost a large part of its intensity in the evening of the 7 November.”

L360: an important conclusion you could mention here is the negligible role of currents.

The negligible impact of the currents was mentioned l. 277, l. 294, l. 310. We add a sentence at the beginning of the discussion “Coupling with the surface currents has no significant impact of the simulation”. We also add a short sentence “Surface currents have no impact” in the abstract.

L384: the gradient of wind speed . . . between which levels?

We changed the sentence to “ the wind speed at first level with respect to the sea surface”.

L385: I suggest to reformulate as “humidity at saturation with temperature equal to SST”.

Yes, done.

L394-398: this part is already discussed and can be omitted.

Yes, removed.

L410-411, L421: This is partly due to the conditional sampling . . .: explain better.

What was meant here is that the lower tail is cut by the high-pass filtering. We added “ as low fluxes are cut off by the sampling” and hope this is clearer.

L424-425, L439: The sentences “The time evolution of the distributions of LE and the SST are opposite to each other” and “parameters controlling LE (and evaporation) are the SST . . . with very strong positive correlations” do not contradict somehow each other?

Yes. The first sentence was misleading, and is a (classical) confusion between apparent correlation and causality, so it has been removed. Thank you for that!

L442: please change “globally” into “positive”.

This paragraph has been removed, due to a major comment of Reviewer #2.

L442-443: this sentence is not clear; my interpretation is that you should rearrange in something like: “The fact that r is low in the whole domain, and higher in EF600 suggests that strong evaporation controls specific humidity and temperature”.

This part has been re arranged due to comments of Reviewer #2, and this sentence has been removed.

L448-449: see major point.

We hope that the reply to this major point is convincing.

L485: in contrast . . .

Change done

L485-486: again, see major point.

We hope that the reply to this major point is convincing.

L531: . . .lack diabatism . . .: really, the second case discussed in Miglietta and Rotunno (2019) does not lack diabatism, but contains both diabatism and baroclinic processes. Please clarify this point here and later in the discussion (L561-564 should be changed, as the Mediane apparently belongs to the second category of Medicanes).

The sentence has been changed and now reads: “Medicanes of the second category also present similarities with tropical cyclones, like deep warm core and symmetrical wind field, but present both diabatism and baroclinic processes”. We also make clear later on in the discussion that “This suggests that the mediane of November 2014 as simulated in this study presents characteristics close to an extratropical cyclone, or mediane of the second category as in Miglietta and Rotunno (2019).”.

L555: This is consistent with the observations in Miglietta et al. (2013) and Dafis et al. (2018).

We added a sentence at the end of this paragraph “The convective activity is stronger during the development than during the mature phase of the cyclone, resulting in heavy rainfall 12 to 6h before the maximum wind speed, in consistency with previous studies of medicanes based on observations (Miglietta et al., 2013; Dafis et al., 2018).”. Also, a figure has been added (Fig. 7) to compare the mean rainfall rates between the development and mature phases.

Figure 6 is very confusing: the coastline can be hardly identified; latitude and longitude are not reported; the extension of the cross section in b) is not clear; finally, the same color scale should be used in both panels. Similar considerations apply to Figure 7.

Yes, we realized that these figures are not easy to read. Fig. 6 has been removed, as we felt it not necessary to the argumentation, and Fig. 7 (now Fig. 11) has been simplified to keep only the necessary information: equivalent and potential temperatures, wind, SLP and strong convergence. Also, the coastlines have been made easier to see and the latitudes/longitudes have been added.

Figure 9: how long do the backtrajectories go back in time?

They start at the beginning of the D2 simulation, at 00 UTC on November, and this is now specified in the caption.

Figure 10: the cyan and blue columns are difficult to distinguish.

We increased the shift between those and we hope this is easier to read.

Figure 11: the triangles are difficult to identify.

We increased the symbol size.

Major comments 1) I find that the technical language used to describe atmospheric dynamics in several parts of the text comes at the cost of a clear interpretation of cyclone dynamics. Here are several examples from the abstract and introduction. I suggest a more careful revision of technical language throughout the text.

Yes, we realized that there was plenty of unnecessary technical vocabulary, especially in the Introduction and Section 3 describing the chronology of the event, and that it does not help to describe the cyclone dynamics. We tried to rephrase this. Thank you for your careful rereading.

line 10: "Tropicalization". I am aware of "tropical transition" but I am afraid I am not familiar with this term. What is its physical/dynamical content? If this term has been used before, then its physical content could be very briefly explained alongside with a reference, if not then, maybe it should be defined in the text.

Tropicalization was used in the paper of Carrio et al., 2017: "Tropicalization process of the 7 November 2014 Mediterranean cyclone: numerical sensitivity study". It is maybe not very common, so it has been replaced by tropical transition as suggested.

line 10: ".. then to low-level convergence and uplift of conditionally unstable air masses by cold pools..". Is it meant that "tropicalization" is a product of jet crossing and latent heat release? Then from the perspective of cyclone dynamics maybe it should be mentioned that both baroclinic and diabatic forcings act in synergy to deepen the cyclone.

Done, thank you for suggesting that, it now reads: "The deepening and tropical transition of the cyclone results from a synergy of baroclinic and diabatic processes".

line 12: "...feeding the latent heat release during the mature phase of the medicane..." do you mean that specific conditions favour convection, in turn leading to high latent heat release? Such phrases were found in several other parts of the manuscript.

This has been rephrased to: "Backtrajectories show that air-sea heat exchanges moisten the low-level inflow towards the cyclone centre".

line 40: A PV streamer is filament of high PV flow it may not be always regarded as equivalent to a trough.

We made it clearer, using "an elongated upper-level trough".

line 40: "potential vorticity (PV) from higher-latitude regions.." you mean intruding stratospheric air characterized by high PV values?

This has been rephrased to: "cold air with high values of potential vorticity"

lines 40-43: I am not sure how these lines help us understand the contribution of different processes in medicanes development.

We wanted to introduce the discussion on the processes due to the specificities of the Mediterranean in the medicane lifecycle, so we listed several geographic factors contributing to their development.

The sentence has been made clearer: “From these studies, a feature common to many medicanes is the presence of an elongated upper-level trough (also known as a PV streamer) bringing cold air with high values of potential vorticity (PV) from higher-latitude regions. Other local effects favouring their development are: lee cyclones forming south of the Alps or north of the North African reliefs (Tibaldi et al., 1990); impact of the coastal reliefs in triggering deep convection; and relatively warm sea surface waters able to feed the process of latent heat release during their mature phase.”

line 46: what do you refer by "upper-level thermodynamics". What is meant by "limited", maybe you mean "inadequate"?

Yes, this sentence was not clear. We rephrased to “It is nevertheless inadequate to describe the respective roles of upper-level and low-level processes (e.g. surface heat exchanges or role of geographical conditions like orographic lifting).”

Line 49: "behaviour", "extension", "..various characteristics" please be specific by rephrasing or attributing a physical content to each term. Please also note that Fita and Flaounas (2018) that warm seclusion may be diagnosed as a warm core symmetric system even if convection is weak. This is opposed to tropical cyclone dynamics.

Yes, this has been changed to “a large diversity of duration, extension (size and vertical extent) and characteristics (dominating role of baroclinic versus diabatic processes)”. We are aware that warm cores may exist as a result of warm air seclusion, this is why we used backtrajectories to check that air is warmed first by air-sea enthalpy fluxes then during convection (diabatic process).

Line 53: "PV transfer from above" I am not sure what is meant here. Do you suggest that a cyclone was intensified due to the formation of a PV tower after aligning air of stratospheric origin with diabatically produced PV in the lower to mid troposphere?

Yes, but the formulation was not clear. It now reads: “rapid deepening of the surface low-pressure system by interaction between low troposphere and upper-level PV anomalies”

Line 56: As formulated here it seems that the PV streamer and the upper level Jet are two different atmospheric features.

Yes, we agree that the formulation was misleading. We reformulated to “Recently, the ubiquitous presence of PV streamers and their key role..”.

Line 60: "large diversity of characteristics and behaviours". Please provide physical content to these words.

This sentence and the following one have been replaced by “They concluded also that, during their lifecycle, medicanes can rely either on purely diabatic processes or on a combination of baroclinic and diabatic processes.”

Line 61-62: I am not sure I understand this phrase. In main lines PV anomalies in a given location can originate from advection (adiabatic process) or from momentum/heat exchanges with the environment (diabatic). Both contribute to the formation of a PV tower and thus both provide a combined baroclinic or diabatic forcing to cyclonic circulation.

Please see above.

Lines 74-77: This phrase is long and difficult to understand.

This has been rephrased: “Turning off the surface turbulent fluxes during different phases of the cyclone brought contrast to this view, showing that the role of surface enthalpy in feeding the cyclonic circulation is not constant throughout its lifecycle. Indeed, it revealed important during its earliest and mature phases, playing only a marginal role during the deepening (Moscatello et al., 2008, case study of September 2006).”

Line 76: please note that atmospheric processes (e.g. convection, or baroclinic instability) are expected to form, or sustain a vortex/cyclonic circulation not enthalpy or surface thermodynamical variables. What is meant here is that surface processes enhance convection and thus a diabatic forcing to cyclonic circulation?

Yes, we made it clearer with “ the role of surface enthalpy in feeding the cyclonic circulation”.

Lines 82-83: "WISHE-type vs baroclinicity". Please rephrase. Baroclinicity is not a mechanism is an atmospheric state.

Yes, we rephrased to “baroclinic processes”.

Lines 83-84: It is quite awkward to characterize a PV-streamer as "instability aloft". Do you mean that stability decreases within the atmospheric column under the PV-streamer?

We rephrased to “ high upper-level PV values”.

Lines 85-86: I am not sure I follow the rational here. Fita and Flaounas, (2018) present a detailed analysis of the implicated dynamics in the development of the december 2005 case. Both a PV-streamer and a cut-off low were involved (the former evolved to the latter). Both features correspond to a PV anomaly of stratospheric origin (cut-off or streamer) that provide a baroclinic forcing to the cyclone. I would say that the difference comes from the extent that baroclinic or diabatic forcing (basically latent heat release due to convection) prevails in provoking cyclonic circulation.

What was meant here is that in the first case, the upper-level PV anomaly above the cyclone centre was connected to the large-scale environment, while it was isolated as a cut-off low in the second case. We agree that a medicane can present both features at different stages of its lifecycle (as this is the case in the present study), and we removed this part of the sentence, as it was misleading and not necessary.

Lines 82 & 87: "WISHE-type" and "WISHE-like". Please be consistent on the terminology. If the mechanism explained here diverges from the original WISHE, please be more specific.

The terminology has been homogeneized, thank you for checking.

Lines 87-88: I do not understand how warm seclusion "replaces" the "heat and moisture to latent heating through a WISHE-like mechanism". Is it meant here that the low-level warm core in the first case is due to convection and latent heat release, while in the second case it is due to warm seclusion?

Yes, this is what was meant. We rephrased to “In the case of October 1996, the cyclone warm core is formed by latent heat release fed at low level by heat and moisture extracted from the sea. In the December 2005 case, the warm core is due to warm air seclusion.”

Line 90: Would you agree that the "Jet-crossing" mechanism refers to a baroclinic forcing to the cyclone? E.g. Jet-crossing could deepen a cyclone even in the absence of any diabatic processes. This seems to be similar to the upper tropospheric forcing " $D\Phi$ " on the medicane case of 2005 in Fita and Flaounas (2018), their Figure 7.

Yes, we agree with that. The sentence has been removed, as confusing and not necessary.

Line 98: Intensity may change due to processes such as convection, not surface heat fluxes. A warmer SST would suggest enhanced convection or at least, favour latent heat release.

Yes of course, but enhanced convection may result from higher CAPE values at low level, due for instance to stronger enthalpy fluxes at the surface. This was simplified to "warmer (respectively colder) SSTs lead to more (resp. less) intense cyclones"

Line 108: Please also note that the impact of coupling has limited effect on "all intense Mediterranean cyclones". This was shown in a simulation ensemble by Flaounas et al., (2018). This could reinforce the argument that known medicane cases are not expected to have an exceptional sensitivity to air-sea coupling than the rest of the intense cyclones.

Yes. The results of Flaounas et al. (2018) are consistent with those of Gaertner et al. (2017), but the latter authors mentioned that this lack of impact can be due to the relatively low resolution of the simulations they compared. If we understood correctly, the simulations used in Flaounas et al. (2018) have also resolutions between 18 and 50 km. We added the reference.

2) Medicanes definition and relevance with this case: A major drawback in the field is the lack of a physical definition for medicanes. I am not sure that it has ever been shown that there is a "perfect vertical alignment between the sea level pressure (SLP) minimum". I could argue that in several papers there is no such alignment observed, especially when the "eye" is fully developed.

Yes, vertical alignment is more a sufficient than necessary condition, and this part of the sentence has been removed.

In line 30 how is radius defined?

We referred here to radius of maximum wind as for the tropical cyclones. We realized that there is probably not appropriate, several authors using the radius of warm core anomaly at 600 hPa for instance. We changed this to "radius" and added the citation of Picornell et al. (2014) as a reference on the typical size of medicanes.

I suggest a more careful opening paragraph mentioning that knowledge comes for a very limited number of cases qualified as medicanes where no objective criteria have been used other than some arbitrary visual characteristics of cloud coverage. After all, several papers show that medicanes present a high variability of dynamical structures (e.g. Miglietta et al., 2017).

Yes, a paragraph on that has been added in the beginning of the introduction: "The medicane cases confirmed by converging characteristics as those mentioned above represent only a small portion of the Mediterranean cyclones (e.g. 13 over 200 cases of intense cyclones in the study of Flaounas et al., 2015, or roughly one per year). Due to this scarcity, isolating in a definite way the characteristics enabling to separate medicanes from other Mediterranean cyclones proved elusive. A study using dynamical criteria concluded that medicanes are very similar to other intense cyclones, with a slightly weaker upper-level and a stronger low-level PV anomalies (Flaounas et al., 2015). Recent comparative studies (e.g. Akhtar

et al., 2014; Miglietta et al., 2017) showed a large diversity of duration, extension (size and vertical extent) and characteristics (dominating role of baroclinic versus diabatic processes) within the medicane category ”.

In fact, from a climatological context, medicanes are not expected to clearly stand out in terms of dynamics from several other cases that were not "qualified" as medicanes.

This seems to be one of the results for several of the metrics used by Tous ad Romero (2013) and Flaounas et al., (2015) in line 37.

Yes, we hope that the previous paragraph makes that clear.

3) I believe that cyclone dynamics in section 3 are not convincingly addressed (this also concerns section 5). It seems to me that this is also partly due to how technical language is used (comment #1).

In summary a PV streamer intrudes the Mediterranean, it provokes cyclogenesis and wraps around the cyclone centre until it evolves to a cut-off at 300 hPa (this is not very clear due to the domain size in figure 5). This scenario seems to be fairly similar to the 2005 medicane, analysed by Fita and Flaounas (2018) and Miglietta and Rotunno (2019), but also to several other cases.

In the "transitional" phase (Fig. 5b), the main body of the PV anomaly is dislocated with respect to the cyclone centre and overall I would say that this example complies with the classic paradigm of baroclinic instability in Hoskins et al., (1985), as illustrated from a PV perspective. What do you refer to with "no trace of baroclinicity" in line 265? With such high PV anomalies in the upper troposphere, the potential temperature isosurfaces should slope accordingly, creating a baroclinic environment to the proximity of the cyclone.

We meant that the frontal structures at low level were not detectable anymore, but we agree that this is a shortcut. We rephrased the sentence to “The medicane presents the circular shape typical of tropical cyclones with spiral rainbands, and a warm, symmetric core (Fig. 5d) extended up to 400 hPa (Fig. 6).”

The analysis in 3.1 is based on the PV-streamer evolution, which mainly refers to adiabatically advected stratospheric air masses. Why do you refer to the last phase of the section as "diabatic"?

How can rainfall be indicative of diabatic vs baroclinic forcing to the cyclone intensification?

We meant here that the heavy precipitation are due to deep convection, which is co-localized with strong PV anomalies at low level and should correspond to with latent heat release (diabatic process), but we agree that this is a shortcut, and contradictory with the heaviest precipitation occurring during before this phase. The description of the chronology of the medicane has been shortened and this sentence has been removed.

Actually the presence of high PV anomaly in the upper troposphere suggests a considerable forcing to the surface cyclone.

Yes, we were referring to the low-level processes here.

Figures 6 and 7 are overcharged and not consistent in the plotted fields. It is also quite odd to use potential temperature at surface level. If this is a model diagnostic (e.g. as 2-meter temperature) rather than a prognostic variable, then it is not used by the model to resolve dynamics. This would create some inconveniences in the analysis.

Furthermore, the field is strongly influenced by land-sea transitions. I suggest you use 850 hPa for low level baroclinic structures. Finally, the two overlaid temperature fields in Fig. 7 makes interpretation of dynamics rather difficult.

Figure 6 appears not necessary and has been removed. We kept Fig. 7 (now 11) to show the role of the cold pools created from rain evaporation or advected from North Africa is initiating the convection. It has been simplified to show only the necessary fields, namely the equivalent and potential temperatures (we felt that these two fields superimposed are actually useful to demonstrate the effect of the cold pools, see of the major comments of Reviewer #1), the SLP, surface wind and strong low-level convergence. It also shows the vertical extension of the cold pools. The potential temperature is a prognostic variable of the model, but equivalent potential temperature and virtual potential temperature are diagnostic. We chose to look at the temperatures at the first level of the model to represent the horizontal extension of the cold pools.

Lines 274-275 "baroclinic processes are responsible for the heavy precipitation" I am not sure I understand this phrase. Are you suggesting that large scale, quasi-geostrophic forced ascent provokes rainfall?

We meant that the frontal structures present at the beginning of the simulated medicane result in convergence and ascent of warm and moist air masses, then in precipitation. This can be interpreted as large-scale rather than more local forcing, but also as baroclinic (frontal) rather than barotropic (e.g. orographic) forcing.

The formulation is now "The heavy precipitation obtained during the first hours are co-localized with frontal structures."

Section 3.1.3: I do not really understand the term "diabaticism". If you refer to the mechanism of tropical transition (Davis and Bosart, 2004) then I guess that you suggest that an initially baroclinic system is now maintained due to convection (as stated in line 316). However there is still an upper PV anomaly due to the streamer. How much does it contribute to the surface cyclonic circulation (also evident in the PV profiles of Fig. 18)?

Yes, the upper level PV anomaly is present throughout the whole event, and it likely contributes to the cyclonic circulation down to the surface, but this has not been quantified, as the main subject of the study is the role of the coupling with the sea surface and the role of the different surface parameters in controlling the enthalpy fluxes.

Does the absence of divergence in the upper troposphere suggest that the dynamics are different from the ones expected by tropical cyclones (lines 313)?

Yes.

It seems that the trajectories "confirm that the warm core of the medicane is actually due to diabatic processes. (lines 330-331)". How do high θ_e values (regardless the origin of these values) assure that the cyclone is maintained due to diabatic forcing?

Equivalent potential temperature (θ_e) should remain constant if condensation takes place. Here, air masses experience a dramatic increase of θ_e . Does this reflect an increase in heat fluxes or moisture?

High θ_e values do not ensure that the cyclone is maintained due to diabatic forcing. Here we follow some particles experiencing heating (increase of θ_e) first at low-level when in areas of strong surface enthalpy fluxes (south and east of Sicily), then when uplifted by deep convection. We did not demonstrate quantitatively that this is due to diabatic heating, and the value of this heating. We

corrected this by assessing the respective changes in humidity (mixing ratio) and potential temperature along the trajectories. During the “surface enthalpy flux stage” i.e. when the particles are close to the surface (between 250 m and 1000 m above sea level), the potential temperatures decrease ($-1\text{ }^{\circ}\text{C}$ in average for the particles show Fig. 17) while the mixing ratio increases of 4.5 g kg^{-1} in one case, 2 g kg^{-1} in the 2 other cases. This shows that the change of θ_e is due to latent heat flux (evaporation) at the surface. During the convective stage, when the particles are uplifted from a few hundreds meters to 1500 m, their mixed ratio decreases of 2 g kg^{-1} and their potential temperature increase of 3.5 to $5.4\text{ }^{\circ}\text{C}$ (condensation and heating, which can reasonably be interpreted as latent heat release). We added a paragraph on that in the text, with the figures mentioned above.

Furthermore, how often do the air masses hit the ground and what is the time interval used to calculate the trajectories? Could you comment on how the method used to calculate the trajectories assures that the "same" air mass is followed in time (especially given the sudden change of altitude after leaving the Sicilian coast)?

Particles followed by the backtrajectories module, in this case, do not hit the ground, they travel between 200 m and a few km. The method used here is based on a passive tracers method (Gheusi and Stein, 2005) inspired by the work of Schär and Wernli (1993). The reference has been added in the text. Backtrajectories enable to follow the same particle from the start of the simulation to this end. It does not ensure, of course, that this particle does not experience transformation, like a change of its potential temperature, humidity, or state.

In fact, factor separation technique in Carrio et al., (2017) shows that the development of this cyclone is due to synergy between upper tropospheric forcing and latent heat release (their figure 14). Could you compare and discuss with respect to their results?

Indeed, the study Carrio et al. (2017) concludes that the upper level PV anomaly is a key process in the preconditioning phase, and that the synergy between this and the latent heat release leads to the rapid deepening of the event. Our conclusions are close to those, and we added a paragraph on that in the discussion: “Finally, these results are consistent with those of Carrio et al. (2017). By using a factor separation technique, they show that while the role of the upper-level PV anomaly is crucial in preconditioning the event, its rapid deepening is due to the synergy of latent heat release and upper-level dynamics”.

4) I suggest to reorganise the manuscript structure to make it more attractive to the reader. Section 4 is very intensive, the importance of the results is eclipsed by a plethora of diagnostics and variables and seems quite detached from section 3. I would suggest to the authors to make a clearer and more refined presentation of the objectives in the introduction and merge the sections 3 and 4 by organising the document sections according to cyclone phases. In fact, section 5 seems to include quite interesting analysis that would be more adequate for section 3.

Yes, this proved to be a very useful comment, helping us to clarify the presentation of the results and to discriminate between our main and secondary results. We re organize the manuscript with only a short description of the chronology of the event in Section 3, more objectively derived from the upper-level and low-level dynamics as in Fita and Flaounas, and completed by the Hart (2003) diagram. We keep in this section the analysis of the SST evolution and of its negligible impact on the medicane. We re arrange Section 4 to include both the results on the control of the surface heat fluxes by the parameters and a more detailed description (than in Section 3) of the different phases of the event. This description is both shorter and more quantitative than is the previous version of the manuscript. Especially, we keep mainly what is related to the low-level processes, and necessary to understand the progress of the medicane. We use the temperature and humidity evolution in a separate way along the particles

trajectories (see above) to check that latent heat release is actually one of the processes of this medicane.

Minor comments:

Abstract: One important message is that intense air-sea interactions have not a strong effect on the cyclone development. Please further highlight your main results, I am not sure about what message we get from lines 16-21.

This has been rephrased as “Analysing the surface enthalpy fluxes shows that evaporation is controlled mainly by the sea surface temperature and wind. Humidity and temperature at first level play a role during the development phase only. In contrast, the sensible heat transfer depends mainly on the temperature at first level throughout the medicane lifetime.”

Line 131: It seems from Di Muzio et al., (2019) that the occurrence of Qendresa was well predicted by ECMWF with a lead time of 7-8 days in contrast to most medicanes, where predictability seems to be possible only in earlier lead times. Could you please comment, or be more specific, on the predictability of this case?

Indeed, the work of Di Muzio et al. (2019) concluded that Qendresa showed a good predictability as early as 7.5 days lead time (LT). This predictability is defined in their paper as the probability of occurrence of the cyclone, based on the ensemble forecasts, with respect to the operational analysis results. They also assessed the predictability of other parameters, like the position, the central pressure, the symmetry, compactness and upper-level thermal wind, mentioned as “the most relevant parameter in distinguishing TLC from fully baroclinic cyclones”. In the case of Qendresa, they obtain a “position forecast jump” (increase of the number of members correctly representing the position of the cyclone during its intense phase) at 4 days LT, but their median position error increases when the LT decreases, to reach a relative maximum at 1 day LT (their Fig. 6), close to the starting time of our D1 simulation. This is consistent with the poor quality of the simulated track we obtained both in the D1 and D2 simulations. Also, the central pressure they obtain (Fig. 4) is ~ 10 hPa higher in average than the analysed one, and they note that “storm intensity forecasts [are] showing little convergence towards the analysis value for Qendresa”. We added the following paragraph in the text: “A recent study based on the ensemble forecasts of the ECMWF (Di Muzio et al., 2019) showed that the predictability of occurrence (with respect to the operational analysis) is good as early as 7.5 days lead time, but the predictability of the position is weak, especially between 4 and 1 days lead time (their Fig. 6). The predicted central pressure is also consistently 10 to 14 hPa higher than the analysed one, whatever the lead time considered”.

Line 213: Typically trajectories refer to air masses and tracks to cyclones. What "best-track" refers to and what kind of observations were used?

The best track, in the present case as in the study of Carrio et al. (2017) was derived from the SEVIRI 10.8 μm channel brightness temperature, this is now specified in the text. Also, the confusion between track and trajectory has been corrected.

Line 226-227: This is contradictory statement please rephrase. In fact, the northward displacement of the track only allows to confirm an agreement of the deepening phase of the cyclone between observations and model.

This has been changed to “The simulated cyclone nevertheless shows a deepening and maximum intensity close to the observed ones”.

Line 239: I do not follow the reasoning of using 100 km radius, been "fitted to the radius of maximum wind". The 100 km radius used is too small, compared to the size of the cyclonic circulation. This is quite clear from the wind field in e.g. Fig. 6. Therefore it seems quite difficult for the diagnostic to capture asymmetries due to frontal structures, which in turn develop in higher length scales. Could you please comment on this?

The cyclone size (defined as the radius of maximum wind at 850 hPa) strongly decreases between the beginning of the development phase and its end (as soon as the cyclone gains its circular shape). To be consistent with the mature and decay phases, we chose the 100 km radius, close to the radius of maximum wind (90 km). As a result, the structure of the cyclone is not well represented by the Hart (2003) diagram during the first part of the development phase, this is why we use the upper-level and low-level dynamics as in Fita and Flaounas (2018) to characterize the time evolution of the cyclone, rather than the Hart (2003) diagram. We added a comment on the size issue in the text: "Please note that the radius of maximum wind is ill defined or larger during the first stage of development of the cyclone, whereas it is steady and close to 90 km during the major part of its lifetime. As a result, the diagram obtained is probably not representative of the cyclone structure during its first hours."

Furthermore Di Muzio et al., 2019 used the operational analyses and same set-up for cyclone phase diagrams and argues that Qendresa presented no warm-core in the upper troposphere. Could you comment on the sensitivity of phase diagrams in your case?

We suggest that the phase diagram representation is sensitive to the model resolution. In the case of the operational analyses used in the work of Di Muzio et al. (2019), the horizontal resolution is 16 km and, given the small size of this event, this could explain the low value (-14) of the upper-level thermal wind in the operational analysis. They note however that [Qendresa] "is widely recognised as a Mediane".

Figure 4 Legends in all axes seem to mention the same pressure layers.

Yes, this was a typo and has been corrected.

Line 360: Could you please comment more on the reasons why cooling may be higher or lower depending on the case and/or location?

We added the following sentences: "Such a discrepancy with a storm of comparable intensity cannot be explained easily, and this is beyond the scope of the present work. A possible explanation could be the storm track affecting the same place by making a loop in the Gulf of Lion, resulting in a larger cooling. The difference can also come from a different oceanic preconditioning (their case occurred in May), with stronger stratification or a shallower mixed layer in the Gulf of Lion that amplifies cooling due to mixing/entrainment process."

References:

- Gheusi, F., and Stein, J.: Lagrangian trajectory and air-mass tracking analyses with Meso-NH by means of Eulerian passive tracers, Techn. Doc., http://mesonh.aero.obs-mip.fr/mesonh/dir_doc/lag_m46_22avril2005/lagrangian46.pdf, accessed on 18/02/2019, 2005.
- Schär, C., and Wernli, H.: Structure and evolution of an isolated semi-geostrophic cyclone. *Quarterly Journal of the Royal Meteorological Society*, 119(509), 57-90, 1993.

Surface processes in the 7 November 2014 medicane from air-sea coupled high-resolution numerical modelling

Marie-Noëlle Bouin^{1,2}, Cindy Lebeaupin Brossier¹

¹CNRM, Université de Toulouse, Météo-France, CNRS, Toulouse, France

²Laboratoire d'Océanographie Physique et Spatiale, Ifremer, University of Brest, CNRS, IRD, Brest, France

Correspondence to: Marie-Noëlle Bouin (marie-noelle.bouin@meteo.fr)

Abstract. A medicane, or Mediterranean cyclone with characteristics similar to tropical cyclones, is simulated using a kilometre-scale ocean-atmosphere coupled modelling platform. A first phase leads to strong convective precipitation, with high potential vorticity anomalies aloft due to an upper-level trough. Then, the deepening and **tropical transition** of the cyclone **result from a synergy of baroclinic and diabatic processes**. Heavy precipitation result from uplift of conditionally unstable air masses **due to low-level convergence at sea**. This convergence is enhanced by cold pools, resulting either from rain evaporation or from advection of continental air masses from North Africa. Backtrajectories show that air-sea heat exchanges moisten the low-level inflow **towards the cyclone centre**. However, the impact of ocean-atmosphere coupling on the cyclone track, intensity and lifecycle is very weak, due to a **sea surface cooling** one order of magnitude weaker than for tropical cyclones, even on the area of strong enthalpy fluxes. **Surface currents have no impact**. **Analysing the surface enthalpy fluxes shows** that evaporation is controlled mainly by the sea surface temperature and wind. Humidity and temperature at first level **play a role** during the development phase **only**. **In contrast**, the sensible heat **transfer depends** mainly on the temperature at first level throughout the medicane lifetime. This study shows that the tropical transition, in this case, is dependent on processes widespread in the Mediterranean Basin, like advection of continental air, rain evaporation **and formation of cold pools**, and dry air intrusion.

1 Introduction

Medicanes are small-size Mediterranean cyclones presenting, during their mature phase, characteristics similar to those of tropical cyclones including a cloudless and almost windless column at their centre looking like a cyclone eye, spiral rain bands and a large-scale cold anomaly surrounding a smaller warm anomaly at their centre, extending at least up to the mid troposphere (~ 400 hPa, **Picornell et al., 2014**). However, they differ from their tropical counterparts by many aspects: their intensity is much weaker, with maximum wind speed reaching those of tropical storms, or Category 1 hurricane on the Saffir–Simpson scale for the most intense of them (Miglietta et al., 2013); their radius ranges typically 50 to 200 km (**Picornell et al., 2014**); due to the enclosed character of the Mediterranean Sea leading rapidly to landfall, and to the limited ocean heat capacity, the duration of their mature phase vary from a few hours to 1 to 2 days; they are able to develop and sustain over sea surface temperature (SST) typically 15 to 23 °C (Tous and Romero, 2013), much colder than the 26 °C threshold of tropical cyclones (Trenberth, 2005; **although tropical cyclones formed by a tropical transition can develop over colder water, McTaggart-Cowan et al. 2015**); and a **development** phase including vertical wind shear and horizontal temperature gradient is necessary to the early stage of their development and the establishment of deep convection (e.g. Flaounas et al., 2015).

In the last decade, several studies documented their characteristics and conditions of formation, either from satellite observations (Tous and Romero, 2013), climatological studies (Flaounas et al., 2015), or case studies based on simulations (Miglietta et al., 2013; 2017; Miglietta and Rotunno, 2019). **From these studies, a feature common to many medicanes is the**

presence of an elongated upper-level trough (also known as a PV streamer) bringing cold air with high values of potential vorticity (PV) from higher-latitude regions. Other local effects favouring their development are: lee cyclones forming south of the Alps or north of the North African reliefs (Tibaldi et al., 1990); impact of the coastal reliefs in triggering deep convection; and relatively warm sea surface waters able to feed the process of latent heat release during their mature phase. Among Mediterranean cyclones, the classification of Hart (2003) established for tropical cyclones and adapted to the Mediterranean conditions (Picornell et al., 2014), helps to reliably identify warm core, symmetric events. It is nevertheless inadequate to describe the respective roles of upper-level and low-level processes (e.g. surface heat exchanges or role of geographical conditions like orographic lifting).

The medicane cases confirmed by converging characteristics as those mentioned above represent only a small portion of the Mediterranean cyclones (e.g. 13 over 200 cases of intense cyclones in the study of Flaounas et al., 2015, or roughly one per year). Due to this scarcity, isolating in a definite way the characteristics enabling to separate medicanes from other Mediterranean cyclones proved elusive. A study using dynamical criteria concluded that medicanes are very similar to other intense cyclones, with a slightly weaker upper-level and a stronger low-level PV anomalies (Flaounas et al., 2015). Recent comparative studies (e.g. Akhtar et al., 2014; Miglietta et al., 2017) showed a large diversity of duration, extension (size and vertical extent) and characteristics (dominating role of baroclinic versus diabatic processes) within the medicane category.

Despite such a context, the role of the large-scale environment like the PV streamer and of the associated upper-level jet has been the subject of several studies. On a case study in September 2006, it was shown for the first time that the crossing of the upper-level jet by the cyclone to the left exit of the jet resulted in a rapid deepening of the surface low-pressure system by interaction between low-troposphere and upper-level PV anomalies (Chaboureaud et al., 2012). Recently, the ubiquitous presence of PV streamers and their key role in the baroclinic development of the medicanes have been confirmed by a study based on simulations and satellite analyses of several cases of intense medicanes (Miglietta et al., 2017). These studies emphasized the importance of the large-scale conditions prior to the development of the cyclone. They concluded also that, during their lifecycle, medicanes can rely either on purely diabatic processes or on a combination of baroclinic and diabatic processes (Miglietta and Rotunno, 2019).

Conversely, the investigation of the contribution of surface processes has motivated few studies so far. Some of them aimed at assessing the relative importance of surface heat extraction versus latent heat release and upper-level PV anomaly throughout the cyclone lifetime, by using adjoint models, factor separation techniques, or turning off selected processes in sensitivity experiments (Reed et al., 2001; Homar et al., 2003; Moscatello et al., 2008; Carrió et al., 2017). They concluded that, whereas the presence of the upper-level trough during the earlier stage of the cyclone and the latent heat release during its developing and mature phases are necessary to its deepening and maintenance, the role of surface heat fluxes is more elusive. Like in tropical cyclones, the latent heat fluxes always dominate the surface enthalpy processes, with sensible heat fluxes representing 25 to 30 % of the turbulent fluxes prior to the tropical transition, and 15 to 20 % during the mature phase (Pytharoulis, 2018). Early studies using simulations first concluded that low-level instability controlled by surface heat fluxes may be “an important factor of intensification” (Reed et al., 2001, case of January 1982) and that the latent heat extraction from the sea is a “key factor of feeding of the latent-heat release” (Homar et al., 2003, case study of September 1996). Turning off the surface turbulent fluxes during different phases of the cyclone brought contrast to this view, showing that the role of surface enthalpy in feeding the cyclonic circulation is not constant throughout its lifecycle. Indeed, it revealed important during its earliest and mature phases, playing only a marginal role during the deepening (Moscatello et al., 2008, case study of September 2006).

More recently, studies simulating several cyclones suggested that the impact of the surface fluxes on the cyclone are probably case-dependent (Tous and Romero, 2013; Miglietta and Rotunno, 2019). The latter study especially compared the

medicanes of October 1996 (between the Balearic Islands and Sardinia) and December 2005 (north of Libya) using the same modelling platform. Sensitivity studies performed with and without surface fluxes showed contrasted results, which were attributed to the different competing roles played by the **WISHE-like** mechanisms (Wind Induced Surface Heat Exchange: Emanuel, 1986; Rotunno and Emanuel, 1987) versus **baroclinic processes** in the two cases. In both cases, **high upper-level PV values** play a strong role in the initiation of the cyclone. The major difference comes from the role of surface fluxes. In the case of October 1996, **the cyclone warm core is formed by latent heat release fed at low level by heat and moisture extracted from the sea. In the December 2005 case, the warm core is due to** warm air seclusion. The authors concluded that different categories of intensification mechanisms leading to medicanes co-exist. This suggests that mechanisms of transition towards tropical-like cyclones are diverse, especially concerning the role of the air–sea heat exchanges.

As surface fluxes may strongly depend on the SST, a change of the oceanic surface conditions may, in theory, impact the development of a medicane. Several sensitivity studies investigated the impact of a uniform SST change on the cyclone development and lifecycle, for instance to anticipate the possible effect of the Mediterranean surface waters warming due to climate change. Consistent tendencies were obtained on different case studies (Homar et al., 2003, case of September 1996; Miglietta et al., 2011, case of September 2006; Pytharoulis, 2018, case of November 2014; Noyelle et al., 2019, case of October 1996), showing that, as expected, warmer (respectively colder) SSTs lead to more (resp. less) intense cyclones. However, changes of SST by less than ± 2 °C result in no significant change in the **track**, duration or intensity of the cyclone. The impact of coupling atmospheric and oceanic models has been studied mainly using regional climate models on seasonal to interannual time scales. Comparing coupled and non-coupled simulations using a regional climate model showed an impact of the coupling provided the horizontal resolution of the model is at least 0.08° (Akhtar et al., 2014). This resolution proved also necessary to reproduce in a realistic way the characteristic processes of medicanes, including warm cores, and strong winds at low level. Coupled simulations resulted in more intense latent and sensible heat surface fluxes, contrasting with what is usually obtained in tropical cyclones due to the strong cooling effect of the cyclone on the sea surface (Schade and Emanuel, 1999; D'Asaro et al., 2007). This can be due to the use of a 1D ocean model and its limited ability to reproduce the oceanic processes responsible of the cooling. The consideration about the resolution needed to observe an impact of the surface processes was confirmed by the results of Gaertner et al. (2017), or Flaounas et al. (2018). Both studies compares several simulations at the seasonal or **interannual** scale, both coupled and uncoupled and from several regional climate modelling platforms. No clear impact of the coupling on the cyclones **intensity** was evidenced but the authors attributed this lack of impact to the relatively low horizontal resolution of the coupled experiments, between 18 and 50 km. Finally, a case study comparing higher-resolution (5 km) coupled and uncoupled simulations of the medicane of November 2011 showed no strong impact of the surface coupling, with a weak decrease of the SST of 0.1 to 0.3°C and a difference of 2 hPa on the minimum of SLP and 5 m s^{-1} on the surface wind speed (Ricchi et al., 2017). The impact of ocean–atmosphere coupling in high-resolution ($\sim 1\text{--}2 \text{ km}$), convection-resolving models has, to the best of our knowledge, not been assessed yet.

In the present study, we assess the feedback of the ocean surface on the atmosphere of the medicane of November 2014 (also known as Qendresa) over the Strait of Sicily and Ionian Sea using a kilometre-scale ocean–atmosphere coupled model. We investigate the role of the surface processes, especially during the **mature** phase of the medicane, and we examine the role of the different parameters (including SST) controlling these fluxes throughout the lifecycle of the cyclone.

A brief **description** of the medicane, and the description of the modelling tools and simulation strategy are given in Sect. 2. In Section 3, the results of the reference simulation are used to describe the **medicane characteristics and lifecycle with its different phases and to present** the impact of the coupling. The role of the surface conditions **and mechanisms** controlling the air–sea fluxes are assessed **during the different phases** in Sect. 4. These results are discussed in Sect. 5, and some conclusions are given.

2 Case study and simulations

The case study is the Qendresa medicane that affected the region of Sicily on 7 November 2014. It has been the subject of several studies based on simulations, either investigating the role of SST anomalies or the impact of uniform SST change (Pytharoulis, 2018), the respective role of upper-air instability, surface exchanges and latent heat release (Carrió et al., 2017) or the predictability of the event, depending on the initial conditions and horizontal resolution of the model (Cioni et al., 2018). All those studies showed that the predictability of this event and especially of its **track** is rather low, even with high horizontal (1–2 km) and vertical (50 to 80 levels) resolutions of present operational numerical weather prediction (NWP) platforms. A recent study based on the ensemble forecasts of the ECMWF (European Centre for Medium-Range Weather Forecasts, Di Muzio et al., 2019) showed that the predictability of occurrence (with respect to the operational analysis) is good as early as 7.5 days lead time, but the predictability of the position is weak, especially between 4 and 1 days lead time (their Fig. 6). The predicted central pressure is also consistently 10 to 14 hPa higher than the analysed one, whatever the lead time considered.

2.1 The 7 November 2014 medicane

On 5 and 6 November 2014, a PV streamer extended from Northern Europe to North Africa, bringing cold air (-23°C) and **enhancing** instability aloft. A general cyclonic circulation developed over the Western Mediterranean basin while Eastern Mediterranean was dominated by high pressures (Fig. 1a). At low level on 6 November, the cold and warm fronts associated with the baroclinic disturbance reinforced due to a northward advection of warmer and moist air, from North Africa (Fig. 1b). The system moved towards the Sicily Strait and deepened during the night of 6 to 7 November. On the early hours of 7 November, the upper-level PV trough and the low-level cyclone progressively aligned (Fig. 1c), reinforcing the PV transfer from above and the low-level instability. Strong convection developed, with heavy precipitation in the Sicily area. The low-level system rapidly deepened in the morning of 7 November, with a sudden drop of 8 hPa in 6 hours, and evolved to the quasi-circular structure of a tropical cyclone with spiral rain bands and a cloudless eye-like centre. The maximum intensity was reached around 12:00 UTC on 7 November north of Lampedusa (see Fig. 3 for main place names). The system drifted eastwards slowly weakening during the afternoon of the 7 November with a first landfall at Malta around 17:00 then moved northeastwards to reach the Sicilian coasts in the evening. It then continued its decay during the following night close to the Sicily coasts, and lost its circular shape and tropical cyclone appearance around 12:00 UTC on 8 November.

2.2 Simulations

Three numerical simulations of the event were performed using the state-of-the-art atmospheric model Meso-NH (Lac et al., 2018) and the oceanic model NEMO (Madec and the NEMO Team, 2016).

2.2.1 Atmospheric model

The non-hydrostatic French research model Meso-NH version 5.3.0 is used here with a fourth-order centered advection scheme for the momentum components and the piecewise parabolic method advection scheme from Colella and Woodward (1984) for the other variables, associated with a leapfrog time scheme. A C grid in the Arakawa convention (Mesinger and Arakawa, 1976) is used for both horizontal and vertical discretizations, with a conformal projection system of horizontal coordinates. A fourth-order diffusion scheme is applied to the fluctuations of the wind variables, which are defined as the departures from the large-scale values. The turbulence scheme (Cuxart et al., 2000) is based on a 1.5-order closure coming from the system of second-order equations for the turbulent moments derived from Redelsperger and Sommeria (1986) in a one-dimensional simplified form assuming that the horizontal gradients and turbulent fluxes are much smaller than their

vertical counterparts. The mixing length is parameterized according to Bougeault and Lacarrere (1989) who related it to the distance that a parcel with a given turbulent kinetic energy at level z can travel downwards or upwards before being stopped by buoyancy effects. Near the surface, these mixing lengths are modified according to Redelsperger et al. (2001) to match both the Monin–Obukhov similarity laws and the free-stream model constants. The radiative transfer is computed by solving long-wave and short-wave radiative transfers separately using the ECMWF operational radiation code (Morcrette, 1991). The surface fluxes are computed within the SURFEX module (Surface Externalisée, Masson et al., 2013) using over sea the iterative bulk parametrization ECUME (Belamari et al., 2005; Belamari and Pirani, 2007) linking the surface turbulent fluxes to the meteorological gradients and the SST through the appropriate transfer coefficients. The Meso-NH model shares its physical representation of parameters, including the surface fluxes parametrization, with the French operational model AROME (Seity et al., 2011) used for the Météo-France NWP with a current horizontal grid spacing of 1.3 km. In this configuration, deep convection is explicitly represented while shallow convection is parametrized using the eddy diffusivity Kain–Fritsch scheme (Pergaud et al., 2009).

In the present study, a first atmosphere-only simulation with a grid spacing of 4 km has been performed on a larger domain of $3200 \text{ km} \times 2300 \text{ km}$ (D1, see Fig. 2). This simulation started at 18:00 UTC the 6 November and lasted 42 h until 12:00 UTC the 8 November. Its initial and boundary conditions come from the ECMWF operational analyses every 6 h.

As described in the following, this 4 km simulation then provides initial and boundary conditions for simulations on a smaller domain of $900 \text{ km} \times 1280 \text{ km}$ (D2, Fig. 2). This domain extension was chosen as a trade-off between computing time and an extension large enough to represent the physical processes involved in the cyclone lifecycle, including the influence of the coasts. All simulations on the inner domain D2 share their horizontal grid (with resolution 1.33 km) and vertical grid with 55 stretched terrain-following levels, and a time step of 3 s. Atmospheric and surface parameter fields are issued every 30 minutes.

2.2.2 Oceanic model

The ocean model used is NEMO (version 3_6) (Madec and the NEMO Team, 2016) with physical parametrizations as follows. The total variance dissipation scheme is used for tracer advection in order to conserve energy and enstrophy (Barnier et al., 2006). The vertical diffusion follows the standard turbulent kinetic energy formulation of NEMO (Blanke and Delecluse, 1993). In case of unstable conditions, a higher diffusivity coefficient of $10 \text{ m}^2 \text{ s}^{-1}$ is applied (Lazar et al., 1999). The sea-surface height is a prognostic variable solved thanks to the filtered free-surface scheme of Roullet and Madec (2000). A no-slip lateral boundary condition is applied and the bottom friction is parameterized by a quadratic function with a coefficient depending on the 2D mean tidal energy (Lyard et al., 2006; Beuvier et al., 2012). The diffusion is applied along iso-neutral surfaces for the tracers using a Laplacian operator with the horizontal eddy diffusivity value ν_h of $30 \text{ m}^2 \text{ s}^{-1}$. For the dynamics, a bi-Laplacian operator is used with the horizontal viscosity coefficient η_h of $-1.10^9 \text{ m}^4 \text{ s}^{-1}$.

The configuration used here is sub-regional and eddy-resolving, with a $1/36^\circ$ horizontal resolution over an ORCA grid from 2.2 to 2.6 km resolution named SICIL36 (ORCA is a tripolar grid with variable resolution, Madec and Imbard, 1996), that was extracted from the MED36 configuration domain (Arsouze et al., 2013) and shares the same physical parametrizations with its “sister” configuration WMED36 (Lebeaupin Brossier et al., 2014; Rainaud et al., 2017). It uses 50 stretched z -levels in the vertical, with level thickness ranging from 1 m near the surface to 400 m at the sea bottom (i.e. around 4000 m depth) and a partial step representation of the bottom topography (Barnier et al., 2006). It has 4 open boundaries corresponding to those of the D2 domain shown in Figure 2, and its time step is set to 300 s. The initial and open boundary conditions come from the global $1/12^\circ$ resolution PSY2V4R4 daily analyses from Mercator Océan International (Lellouche et al., 2013).

2.2.3 Configuration of simulations

The three-hourly outputs of the large-scale simulation on D1 were used as boundary and initial conditions for 3 different simulations on the smaller domain D2, based on the atmospheric and oceanic configurations described previously. These three simulations start at 00:00 UTC on 7 November and last 36 h until 12:00 UTC on 8 November. The first atmosphere-only simulation called NOCPL used a fixed SST forcing, while the CPL simulation is the two-way coupled simulation between the Meso-NH and NEMO-SICIL36 model. Indeed, in CPL, the SURFEX-OASIS coupling interface (Voldoire et al., 2017) enables to exchange the SST and two-dimensional surface currents from NEMO to Meso-NH and the two components of the momentum flux, the solar and non-solar heat fluxes and the freshwater flux from Meso-NH to NEMO every 15 minutes. To test the respective impact of the surface currents on the atmosphere with respect to the impact of the SST, another coupled simulation has been performed (NOCUR in the following). It is similar to CPL except that the surface currents are not exported from NEMO to Meso-NH.

In order to ensure that the impact of the coupling in the NOCUR and CPL configurations corresponds to the time evolution of the SST rather than to a change in the initial SST field, the SST field (shown in Fig. 3) used as a surface forcing in NOCPL (and kept constant throughout the simulation) is the field produced by the CPL run, 1 h after the beginning of the simulation (i.e. after the initial adjustment of the oceanic model).

2.3 Validation

The tracks of Qendresa obtained in the three different simulations are compared to the best track based on observations (brightness temperature from radiance in the 10.8 μm channel measured by the SEVIRI instrument aboard the MSG satellite, see Cioni et al., 2018) in Figure 3. All the simulated tracks are shifted northwards with respect to the observations since the beginning of the simulations. The mean distance between the simulated and observed tracks is close to 85 km with no significant difference between the simulations. Cioni et al. (2018) showed that using horizontal resolutions finer than 2.5 km is mandatory to accurately represent the fine-scale structure of this cyclone and its time evolution. Sensitivity studies showed an increased convergence of simulated track towards the observations with higher resolution, the best agreement being obtained with a nested configuration and an inner domain at 300 m resolution. In the present study, several sensitivity tests based on these results were performed on the smaller-domain simulation to improve the simulated track: i) the starting time of the simulation was changed between 12:00 UTC on 6 November and 00:00 UTC on 7 November with increment of 3 h; ii) the number of vertical levels in Meso-NH was increased to 100, with a stretching ensuring a better sampling in the atmospheric boundary layer; iii) the atmospheric simulation was performed without nesting, initial and boundary conditions from ECMWF, and horizontal resolution of 2 km. Note that our inner domain D2 is close in its extension to the domain used by Cioni et al. (2018). None of these tests resulted in a significantly improved track, the northward shifting of the cyclone occurring in every case in the early hours of the 7 November.

The simulated cyclone nevertheless shows a deepening and maximum intensity close to the observed ones, even if a direct (i.e. co-localized) comparison is not possible due to the northward shift of its track. A strong deepening of almost 15 hPa is obtained in the first 12 h of the CPL simulation (Fig. 4b) with a minimum value at 12:30 UTC on the 7 November close to the minimum observed at Linosa station. This station has been chosen as the closest point to the best track from observations at the time of the observed maximum intensity of the storm. The surface wind speeds show peak values at the same time (Fig. 4a), and a time evolution in good agreement with METAR observations at the stations of Lampedusa, Pantelleria or Malta. Wind speed averaged over a 50 km radius around the cyclone centre presents a time evolution close to the control simulation of Cioni et al. (2018).

3 Medicane lifecycle and coupling impact

This part presents first the successive phases of the event based on an analysis of upper-level and mid-troposphere processes. Then, the impact of taking into account the short-time evolution of the SST on the atmospheric surface processes, through ocean–atmosphere coupling, is assessed.

3.1 Chronology of the simulated event

The successive phases of the medicane are examined using the methodology of Fita and Flaounas (2018) based on its upper-level and low-level dynamics, and on its asymmetry and thermal wind. Figure 5 shows the 300 hPa PV anomaly, SLP, surface wind and equivalent potential temperature θ_e at 850 hPa from the NOCPL simulation. Moreover, phase space diagrams are commonly used to describe in a synthetic way the symmetric characteristics of the cyclone, as well as the thermal characteristics and extent of its core. The present version in Figure 6 showing the evolution of Qendresa from 01:00 UTC on 7 November to 12:00 UTC on 8 November is derived from the original work of Hart (2003) using the adaptation of Picornell et al. (2014) for smaller-scale cyclones. The radius used for computing the low-troposphere thickness asymmetry B , the low-troposphere and upper-troposphere thermal winds ($-V_{TL}$ and $-V_{TU}$ respectively) has been fitted to the radius of maximum wind at 850 hPa and is close to 100 km, and the low troposphere and upper troposphere are defined here as the 925–700 hPa and 700–400 hPa levels respectively. Please note that the radius of maximum wind is ill defined or larger during the first stage of development of the cyclone, whereas it is steady and close to 90 km during the major part of its lifetime. As a result, the diagram obtained is probably not representative of the cyclone structure during its first hours.

At 06:00 UTC on 07 November, the PV streamer has moved northwards from Libya and is located south of the SLP minimum (Fig. 5a). A south-north cold front is clearly visible in the 850 hPa θ_e , east of the cyclone centre, and the medicane centre is located under the left exit of the upper-level jet (Fig. 5b). The minimum SLP starts to decrease to reach 985 hPa around 11:00 UTC, corresponding to a strong deepening rate of 1.4 hPa hr^{-1} for 10 hours. This phase corresponds also to the increase of the maximum wind at low level, and of the wind speed averaged over a 100 km radius around the cyclone centre (Fig. 4). It is referred to as “development phase” in the following. The heaviest rainfall are obtained during this phase (Fig. 7) with 10 h accumulated rain above 200 mm locally and instantaneous values above 50 mm h^{-1} east of Sicily and at sea between Pantelleria and Malta. As in Fita and Flaounas (2018), it also corresponds to the maximum thermal wind (Fig. 6).

The jet then moves further over the Ionian Sea and Sicily and the SLP minimum is aligned with the 300 hPa PV anomaly at 11:00 UTC on 7 November (Fig. 5c). It corresponds to the beginning of the “mature phase”, with a maximum intensity of the medicane around 12:00 UTC (Fig. 4). The medicane presents the circular shape typical of tropical cyclones with spiral rainbands, and a warm, symmetric core (Fig. 5d) extended up to 400 hPa (Fig. 6). The upper-level PV anomaly stays wrapped around the SLP until 17:00 UTC, and both structures drifts eastwards south of Italy (Fig. 5e). The medicane slowly decreases in intensity (Fig. 4) until its landfall in the southeast of Sicily at 18:00 UTC. The cold front drifts eastwards away of the cyclone centre, evolving eventually into an occluded front (Fig. 5f) wrapped around the SLP minimum. This mature phase, although the most intense of the cyclone, results in more scattered rainfall than the development phase (Fig. 7).

The cyclone then moves northeastwards towards the Ionian Sea and continuously decreases until 12:00 UTC on 8 November (“decay phase” hereafter). The SLP minimum steadily increases (Fig. 4), the upper-level PV anomaly has evolved into a cut-off and is still collocated with the cyclone centre (Fig. 5g). The 850 hPa warm core has extended $\sim 250 \text{ km}$ around the cyclone centre (Fig. 5h).

In the following, the possible impact of the ocean–atmosphere coupling on the cyclone intensity is examined by comparing the results of the CPL, NOCUR, and NOCPL simulations. The time period for this comparison is the 7 November only, as the medicane has lost a large part of its intensity in the evening of the 7 November.

3.2 SST evolution

Taking into account the effect of the SST cooling only (NOCUR) results in a slightly slower and less intense deepening by 1.5 hPa and almost no change of the maximum wind (Fig. 4). Including the effect of the surface currents on the atmospheric boundary layer results in a slightly more intense cyclone (1.5 hPa difference) at its maximum and 8 m s^{-1} stronger maximum wind. Figure 3 shows also that no significant difference on the track is obtained between the NOCPL, NOCUR and CPL simulations, except maybe when the cyclone centre loops east of Sicily at the end of the day. The median values of the difference of the SST between the CPL and NOCPL simulations over the whole domain, and the values of the 5 %, 25 %, 75 % and 95 % quantiles are shown Figure 8. This median surface cooling is very weak and reaches barely 0.1°C at the end of the development phase, and is close to 0.2°C at the beginning of the decay phase. Its further evolution, during the decay phase, is very weak with values of 0.25°C at 23:00 UTC, on 07 November. The maximum cooling is 0.6°C . To focus on the effects of this surface cooling on the surface processes feeding the cyclone, we used a conditional sampling technique to isolate the areas with enthalpy flux above 600 W m^{-2} that corresponds to the mean value of the 80 % quantile of the enthalpy flux on the day of the 7 November. The enthalpy flux is defined here as the sum of latent heat flux LE and the sensible heat flux H . On this area (EF600 hereafter), the SST difference and its time evolution are slightly larger with a median difference of -0.2°C at the beginning of the mature phase and close to -0.4°C at the end of 7 November. The SST difference obtained in NOCUR on EF600 is slightly larger than in CPL but the difference is not significant. The SST cooling on the area of highest fluxes that are responsible for supplying the medicane in heat and moisture is therefore under 0.4°C in median value, and much weaker than typical cooling values observed under tropical cyclones, that commonly reach 3 to 4°C (e.g. Black and Dickey, 2008). In addition, the spatial extent of the cooling does not correspond to a clear wake as in tropical cyclones (not shown).

The conclusion of this part is that surface cooling under this medicane is one order of magnitude smaller than what is obtained under tropical cyclone, with no significant impact of the surface currents. Quantifying the surface cooling under other medicanes could lead to contrasting results. For instance, in an ocean–atmosphere–waves coupled simulation of a strong storm in the Gulf of Lion, surface cooling of 2°C was obtained (Renault et al., 2012). Such a discrepancy with a storm of comparable intensity cannot be explained easily, and this is beyond the scope of the present work. A possible explanation could be the storm track affecting the same place by making a loop in the Gulf of Lion, resulting in a larger cooling. The difference can also come from a different oceanic preconditioning (their case occurred in May), with stronger stratification or a shallower mixed layer in the Gulf of Lion that amplifies cooling due to mixing/entrainment process.

3.3 Impact on turbulent surface exchanges

A comparison of the time evolution of the enthalpy flux, sensible and latent heat fluxes of the NOCPL and CPL simulations shows that the differences are very weak even on the EF600 area (Fig. 9a). During the decay phase where it is maximum, the mean difference of the enthalpy flux is 25 W m^{-2} , with a standard deviation of 13 W m^{-2} . Compared to the values of the turbulent fluxes on this area, between 500 and 800 W m^{-2} for LE and 100 and 250 W m^{-2} for H , this value is weak. Expressed in percent of the fluxes values, the relative difference is close to 2 % at the beginning of the mature phase and reaches 5 % at 21:00 UTC on 7 November, when the medicane has weakened. The relative difference of the sensible heat flux varies between 4 and 10 % due to the lower values of H , and the value of the difference is close to 7 W m^{-2} with a standard

deviation of 4 W m^{-2} . So, coupling appears to have a very weak impact on the turbulent heat fluxes even in the EF600 area. Again, the effect of the surface currents (CPL versus NOCUR in Fig. 9b) is not significant.

In the following, except if otherwise specified, the results of the NOCPL simulation are used to investigate the medicane behaviour, focusing on what occurred area of interest (AI in Fig. 2).

4 Role of surface fluxes and mechanisms

This section investigates the role of the surface parameters in controlling the surface heat fluxes during the different phases of the medicane. The objective is to assess the relative role of the SST, the surface wind, and the heat and moisture in the surface layer in the surface heat transfer and its time evolution.

4.1 Representation of surface fluxes and methods

In numerical atmospheric models, the turbulent heat fluxes are classically computed as a function of surface parameters using bulk formulae:

$$H = \rho c_p C_h \Delta U \Delta \theta \quad (1)$$

$$LE = \rho L_v C_e \Delta U \Delta q \quad (2)$$

with the air density, c_p the air thermal capacity and L_v the vaporization heat constant, ΔU , $\Delta \theta$ and Δq the wind speed at first level with respect to the sea surface, the difference between the SST and the potential temperature at first level, and the difference between the specific humidity at saturation with temperature equal to SST and the specific humidity at first level, respectively. The transfer coefficients C_h and C_e are defined as

$$C_h^{1/2} = \frac{C_{hn}^{1/2}}{1 - \frac{C_{hn}^{1/2}}{\kappa} \psi_T(z/L)} \quad (3)$$

and

$$C_e^{1/2} = \frac{C_{en}^{1/2}}{1 - \frac{C_{en}^{1/2}}{\kappa} \psi_q(z/L)} \quad (4)$$

with κ the von Karman's constant, ψ_T and ψ_q empirical functions describing the stability dependence, C_{hn} and C_{en} the neutral transfer coefficient for heat and moisture and L the Obukhov length (which depends, in turn, on the virtual potential temperature at first level and on the friction velocity u_*). In the ECUME parameterization used in this study, the neutral transfer coefficients C_{hn} and C_{en} are defined as polynomial functions of the 10 m neutral wind speed.

The transfer coefficients depends on the wind speed at 10 m and on the Obukhov length through the stability functions. The Obukhov length is expressed as in Liu et al. (1979):

$$L = - \frac{T_v^2 u_*^2}{\kappa g T_{v*}} \quad (5)$$

with T_v the virtual temperature at the first level, depending on the temperature and specific humidity, and T_{v*} the scale parameter for virtual temperature depending on the temperature and humidity at the first level. As a consequence, the transfer coefficients depend as the fluxes on the wind speed, on the temperature and specific humidity at the first level, and on the SST. In the following, we do not distinguish between the temperature and potential temperature at first level.

The time evolution of the median values, and 5 %, 25 %, 75 % and 95 % quantiles of the latent and sensible heat fluxes is shown in Figure 10a for the 7 November, on the EF600 area, and the time evolution of the median values and quantiles of

the SST in Figure 10b. The latent heat flux is always much higher than the sensible heat flux, as this is generally the case at sea when the SST is above 15 °C (e.g. Reale and Atlas, 2001). The sensible heat flux represents here 22 % of the total turbulent flux during the development phase, 12 to 15 % during the decay phase. Both fluxes show asymmetric distributions with upper tail (95 %) more distant from the median than the lower tail (5 %). This is partly due to the conditional sampling ($LE + H > 600 \text{ W m}^{-2}$) used here, as low fluxes are cut off by the sampling. The median value of H is maximum at the end of the development phase (180 W m^{-2} at 08:00 UTC), while the maximum value of its 95 % quantile is reached at the beginning of the development phase (332 W m^{-2} at 04:00 UTC). During the mature phase, both the median and 95 % quantile values of H are continuously decreasing. Conversely, the maximum of the median value of LE (635 W m^{-2}) is reached at 09:00 UTC during the development phase and stays approximately constant until 15:00 UTC. The maximum of the 95 % quantile (845 W m^{-2}) is reached at the end of the development phase. The decrease of LE starts later than the for H (around 15:00, as the system has started to weaken) and is slower until the end of the 7 November. The median values of LE in this EF600 sampling are constant or slightly increasing until the evening (20:00 UTC), whereas the minimum values (5 % quantile) increase continuously until the end of the day. Again, this is probably partly due to the sampling used here.

The time evolution of the median values and quantiles of the SST shows, conversely, asymmetric distributions with lower tails much longer than upper tails (Fig. 10b). The maximum values of SST (95 % quantile) are almost constant with time and close to 24 °C, while the lower and median values vary due to the conditional sampling EF600 and the motion of the cyclone away from the warm SST area.

To investigate the mutual dependencies and co-variabilities of the fluxes and parameters listed above, we used the rank correlation of Spearman, which corresponds to the Pearson or linear correlation between the rank of the two variables in their respective sampling (Myers et al., 2010). This metrics enables relating monotonically rather than linearly the variables of interest and is more appropriate in the case of non-linear relationships as this is the case for the fluxes that may be related to the variables additionally through the transfer coefficients.

The co-variabilities are analysed first in the whole domain, to determine what contributes the most to the fluxes globally, then in the EF600 area to isolate processes explicitly responsible for the fluxes contributing the most to the growth and maturity of the medicane. The corresponding values are given in Tables 1 to 3 for the EF600 area, and for 3 time periods considered representative of the development, mature and decay phases respectively, i.e. 09:00, 13:00 and 18:00 UTC on 7 November.

4.2 Development phase

At low level, this phase corresponds to a low-pressure system resulting of the evolution of the instability generated by the lee cyclone induced by the North African relief, with strong baroclinic structures. The heavy precipitation obtained during the first hours are co-localized with frontal structures. A warm sector is present at the east of the domain, with a cold front extending south-east from the south of Italy and very strong low-level convergence between a southeasterly flow in the warm sector and a south to southwesterly flow in the cold sector.

At 08:30 UTC on 7 November (Fig. 11), strong convergence lines are present between Sicily and Tunisia, close to the cyclonic centre. The low-level virtual potential temperature θ_v superimposed to the equivalent potential temperature θ_e on the map (Fig. 11a) and on an east-west (E-W) cross section close to the SLP minimum (Fig. 11b) is used here as a marker of cold pools (with an upper limit of 19°C for θ_v – Ducrocq et al., 2008; Bresson et al., 2012). Some of these cold pools are the result of evaporating processes under convective precipitation, while those located at sea along the North African coast originates from dry and cold air advected from inland (the discrimination between these two kinds of cold pools was done using a simulation without the latent heat transfer due to rain evaporation, not shown here). The cold and moist air spreads to the

surface following density currents and is advected northwestwards by the low-level flow. On the west and south of the domain, cold pools were formed at night by radiative processes over land, then advected over sea with a vertical extent of ~ 1000 m (see the westernmost part of the W-E transect, Fig. 11b).

The strong horizontal convergence at low level, leading to uplift and deep convection on air masses with high θ_e , is located on the upwind edge of the cold pools. During this development phase, the cold pools located in the southerly flow move northwards, towards the centre of the cyclone and trigger convection up to 3000 m of the northwesterly low-level flow with high θ_e (Fig. 11b). This propagates the surface warm anomaly close to the cyclone centre (now located under the 300 hPa PV anomaly) up to 3000 m and develops a corresponding low- to mid-troposphere PV anomaly. At the same time, a dry air intrusion from the upper levels brings air masses with low θ_e and relative humidity below 20 % to 3000 m, resulting in a upper-to-mid-troposphere PV anomaly (Fig. 15a and c).

To identify the surface parameters controlling evaporation at sea, the time evolution of the Spearman's rank correlations between the latent heat flux, U_{10} , θ , the SST and q is given Figure 12 and Tables 1 to 3.

During this phase, on the whole domain, the controlling parameters for LE are the SST and the wind (positively correlated), the specific humidity (negatively) and the potential temperature (negatively). Potential temperature and humidity are also strongly positively correlated ($r_s = 0.55$ over the whole domain), due to the advection of cold and dry air by the southerly low-level flow from the Tunisian and Libyan continental surface (Fig. 13b, c and f, at 09:00 UTC). This air mass progressively charges itself in heat and moisture on the area of strongest enthalpy fluxes north of the Libyan coasts (Fig. 13a). The EF600 area of strong fluxes and cold/dry air corresponds also to the area of warm SST (Fig. 13e). Within this area, the main influence on LE is from the wind, then from the SST (Fig. 12b, Table 1). There is no effect of the potential temperature (weak or negative correlations, Fig. 12b, Table 1) and a weak effect of the specific humidity.

LE is always much higher than H (Fig. 10a), resulting in the “strong flux area” EF600 being determined by LE values rather than H values, and more homogeneous values of LE than H over this area. However, H can reach strong values locally with respect to the LE during this development phase. As a consequence, values of H still show strong contrast on the EF600 area (Fig. 13d). During this development phase, it is controlled mainly by the potential temperature at first level (Fig. 14), partly indirectly through the stratification and transfer coefficient (not shown). On the EF600 area also, the SST influence is weak at all times, the major control is also from the potential temperature ($r_s = -0.70$ at 09:00 UTC). The wind plays a secondary role. The enhanced control by the potential temperature is partly due to the continental air masses advected from North Africa, and partly to the presence of the cold pools under the areas of deep convection and strong wind. The H values are located offshore of the Tunisian and Libya coasts downwind of the strong low-level flow bringing cold air from the continent.

4.3 Mature phase

At 13:00 on 7 November, the PV anomalies at 700 hPa and 300 hPa are aligned (Fig. 15c, e). A zonal cross section on the SLP minimum shows that a low-level PV anomaly with values above 5 PVU has formed around the centre of cyclone, extending from the surface up to the 300 hPa anomaly (Fig. 15). The warm core of the systems extends up to 850 hPa (Fig. 15a), and is limited upward by colder air (low θ_e) brought from aloft. The tangential velocity field shows low-level convergence (up to 800 hPa) towards the cyclone centre, deep convection close to the centre, but no or very weak divergence at mid to upper troposphere. The cyclonic circulation has reinforced with horizontal wind speed above 8 m s^{-1} at all heights out of a radius of 10 km around the cyclone centre.

During this phase as the previous one, over the whole domain as in the EF600 area, the dominant role in controlling evaporation is played by the SST with an effect equivalent to the wind speed, and a decreasing influence of the humidity

(Fig. 12, Table 2). The area EF600 extends further north, closer to the cyclone centre, away from the area of cold and dry low-level air, which also tends to warm and moisten under the combined impact of the diurnal warming of the continental surfaces (not shown) and of the strong enthalpy fluxes offshore (Fig. 16a, c and f). The sensible heat flux is still controlled by the temperature, with an increasing influence of the wind.

4.4 Decay phase

In the afternoon of the 7 November, the cyclone first moves towards colder SSTs in the east of the Sicily Strait (Fig. 3), then crosses Sicily and reach the Ionian Sea around 20:00 UTC, with even colder SSTs, before slowly decaying and losing its tropical-like characteristics. To check the role played by warm and moist air extraction from the sea-surface in feeding the cyclone centre by air masses with high θ_e values, backtrajectories were used starting at 23:00 on the 7 November, south of the cyclone centre (Schär and Wernli, 1993; Gheusi and Stein, 2005). The trajectories of three air parcels originating from very different places and arriving at the same place, at three vertical levels surrounding the level closest to 1500 m, are shown in Fig. 17. Their equivalent potential temperature ranges from 31 to 38 °C at their first appearance in the domain and is close to 45 °C on average when they reach their final point. On their trajectories, θ_e increases almost continuously, with a strong jump during their transit at low level (below 500 m) above the sea in the EF600 area (white contour in Fig. 17). A separate analysis of the two different stages of the trajectories has been performed. Stage 1 corresponds to the particles in the low-level flow (between 200 and 1200 m above sea level) south and east of Sicily and stage 2 to their convective ascent from ~ 300 m to 1500 m. During stage 1, the potential temperature of the particles decreases of 1 °C in average while the mixing ratio increases of 2.8 g kg⁻¹. This shows that the increase in θ_e is due to strong surface evaporation. During stage 2, the mixing ratio of the particles decreases of 2 g kg⁻¹ and their potential temperature increases of 4.1 °C. This indicates condensation and latent heating. This demonstrates the strong role of the sea surface in increasing the moisture and heat of the low-level flow before its approach of the cyclone centre, and of diabatic processes in reinforcing its warm core.

During the decay phase, the influence of the humidity on the evaporation, in the whole domain is weak (Fig. 12a). The area of strong enthalpy fluxes is still located on warm SSTs on the south of the domain (Fig. 18a, e), which is also the place of the strongest winds on the right-hand side of the cyclone (Fig. 18b). Within the EF600 area, there is almost no influence of the temperature or humidity on LE (Table 3). The influence of the wind speed is decreasing, the role of the SST is strong until 21:00 UTC when the cyclone reaches the northern Ionian Sea where the SST is much colder, and the effect of the wind speed becomes dominant at the very end (Fig. 12b). Concerning the sensible heat flux, there are less patches of strong flux corresponding to cold pools and low θ , but a medium-scale northwest–southeast gradient of H over the EF600 area, related to a NS gradient of wind speed (Fig. 18b). On the north of the EF600 area (where the wind speed is also the highest), the potential temperature is colder and H values are maximum.

In summary, at the scale of the domain, the latent heat flux (evaporation) is controlled by the SST and wind throughout the day of the 7 November: both strong winds (in the cold sector during the development phase, then close to the cyclone centre and in its right side) and warm SSTs (in the south of the domain) are thus necessary to have strong latent heat fluxes. Within the area where the turbulent fluxes are high (and where winds are strong and SSTs high), the control of evaporation is mainly from the wind (development and mature phases) then from the SST (decay phase). In contrast, the sensible heat flux is always mainly controlled by the potential temperature in the surface layer. Colder air masses result in enhanced sensible heat flux, rather than strong wind or warmer SST. During the two first phases, this cold air is either advected from North Africa or created by evaporation under convective precipitation (cold pools). During the decay phase, strong latent heat transfer over warm SSTs warms the near-surface atmospheric layer and results finally in lower sensible heat transfer.

5 Discussion and conclusion

The comparison of the simulations with and without ocean coupling shows no significant impact of the evolution of the SST on the track, intensity or lifecycle of the medicane. The weak SST cooling, notably during the first 24 h of the simulation, is likely responsible for that. On the strong flux area, where the enthalpy flux feeds the cyclone in heat and moisture maintaining the convection and the latent heat release mechanism, the median value of the SST cooling is 0.2°C during the mature phase, and reaches barely 0.4°C at the end of the day. The median difference on H is -7 W m^{-2} during the mature phase, -12 W m^{-2} at 23:00 UTC on the 7 November (representing less than 10 % difference), and -19 W m^{-2} , -37 W m^{-2} on LE at the same two time periods (representing less than 5 % difference). Coupling with the surface currents has no significant impact of the simulation.

The co-variabilities of surface fluxes and parameters show nevertheless that, in this specific case, the SST exerts a strong control on the latent heat flux that dominates the surface heat transfer, throughout the whole duration of the event. During its development phase, there is also a strong influence of peculiarities of the Central Mediterranean: the transition between deep convection and heavy precipitation associated with baroclinic processes and the tropical-like cyclone takes place downwind of the low-level flow of dry and cold air originated from North Africa. These air masses with low θ_v encounter moist and warm air resulting of the strong sea-surface evaporation and enhance the deep convection at sea, together with the cold pools formed by rain evaporation and downdrafts. These cold pools of various origins displace the deep convection at sea. Uplift of warm air masses increases the low-level PV, and reinforces the vortex, which is moved northeastwards closer to the PV anomaly aloft.

It has recently been suggested that medicanes could be sorted into two (possibly three) different categories according to the intensity and role of air–sea heat exchanges and to the related surface mechanisms (Miglietta and Rotunno, 2019). The main difference between these two categories is the processes leading to the warm core of the cyclone. The first category corresponds to purely WISHE-like mechanisms, with latent heat release fed by heat and moisture extracted from the sea surface as processes responsible for the medicane deepening and warm-core building. The cyclone is detached from any large-scale, baroclinic structure during its mature phase, with no transfer of PV from the upper-level jet. The PV anomaly at all levels consists in: wet potential vorticity (WPV) produced diabatically by latent heat release (Eq. 4 in Miglietta et al., 2017) and dry potential vorticity (DPV) brought by intrusion of stratospheric air into the upper troposphere (their Eq. 3). Levels up to $\sim 600\text{ hPa}$ present a maximum of WPV due to latent heating, while DPV is almost constant up to $\sim 400\text{ hPa}$ where it increases sharply, and there is no real PV tower around the cyclone centre. The features characteristics of tropical cyclones are well marked: warm core extending up to 800 hPa , symmetry, low-level convergence and upper-level divergence, and strong contrast of θ_e ($\sim 8^{\circ}\text{C}$) between the surface and 900 hPa as an evidence of latent heating. The case of October 1996 chosen to represent this category shows very strong surface fluxes (above 1500 W m^{-2} over large areas) due to strong, persistent winds of orographic origin bringing cold and dry air for several days prior to the cyclone development, also contributing to destabilize the surface layer.

Medicanes of the second category also present similarities with tropical cyclones, like deep warm core and symmetrical wind field, but present both diabatic and baroclinic processes throughout their lifetime. The cyclone stays within a large-scale baroclinic environment, with the PV streamer slowly evolving into a cut-off low. The tropical-like features are less evident: weaker warm core, weaker gradient of θ_e ($\sim 3\text{--}4^{\circ}\text{C}$) between the surface and 900 hPa . Around the cyclone centre, a PV tower forms, with weak contrast between the DPV and WPV profiles. As an example, the warm core of the December 2005 medicane is not due to convective latent heating but to seclusion of warm air by colder air masses and extends up to 400 hPa . The surface enthalpy fluxes play only a marginal role and take maximum values of 1000 W m^{-2} for a few hours.

In the present case of Qendresa, strong air–sea exchanges at the surface and latent heat release act at building the warm core anomaly, as seen in Sect. 4.3 and 4.4. The surface enthalpy fluxes take intermediate values with maximum above 1500 W m^{-2} for a few hours on areas with warm SST and strong winds downwind of the dry low-level flow from North Africa. Thermal features characteristic of tropical cyclones are present, like low-level cold air advection from the south to the east, and warm air advection from the south to the north (Reale and Atlas, 2001), and the gradient of θ_e between the surface and 900 hPa takes intermediate values of 6–7 °C. The wrapping of the PV streamer around the cyclone centre evolves into an upper-level cut-off at the end of the decay phase. Conversely, some typical features are not present: even if there is weak low-level convergence around the cyclone centre, no divergence is obtained at upper level. The area of maximum latent heat flux within the EF600 area is more controlled by the SST than by the wind speed (Fig. 12b and 13a, b, and e). No minimum of potential temperature or potential vorticity develop at 300 hPa close to the cyclone centre during the mature phase, as a marker of the PV anomaly erosion by the convective activity, and the upper-level PV anomaly never completely detaches from the large scale structure.

The vertical profiles of PV, DPV and WPV (defined as in Miglietta et al., (2017)) averaged on a 100 km radius circle around the cyclone centre show a minimum of WPV between 700 and 400 hPa during the decay phase, and a clear difference between DPV and WPV at low level (Fig. 19). The DPV is weak up to the mid troposphere and increases sharply above 400 hPa. The WPV anomaly at low levels that develop up to 700 hPa during the development phase is increased but its vertical extent is reduced to 800 hPa during the mature phase (13:00 UTC – see also Fig. 15e). This is due to a dry air intrusion during the mature and decay phases, which is limited downwards to mid troposphere because of this warm core (Fig. 15a). At the beginning of the decay phase, at 18:00 UTC, the latent heating within the cyclone core increases the WPV at low level and erodes the dry and cold (θ_e) air masses up to 650 hPa. The warm core and WPV anomaly extend upwards (Fig 15b, f), and the DPV anomaly is pushed up to 700 hPa (Fig. 15c, d).

This suggests that the medicane of November 2014 as simulated in this study presents characteristics close to an extratropical cyclone, or medicane of the second category as in Miglietta and Rotunno (2019). Its development phase is triggered by a PV streamer bringing instability at upper level, and baroclinic processes followed by strong convection at sea enhanced and maintained by cold pools due to rain evaporation at low level or by advection of dry and cold air from North Africa. Conjunction of advection of continental air masses with evaporation under storms has not been identified as leading to tropical transition of Mediterranean cyclones so far, even though it is probably rather ubiquitous, as both are rather widespread phenomena in the Mediterranean. Surface fluxes are strong and contribute to enhance the convection potential till the mature phase of the cyclone. Evaporation is mainly controlled by the SST and by the wind speed during the whole event, while the temperature difference between the SST and the cold air advected from North Africa during the development and mature phase play a strong role during its development. The vertical development of the warm core is limited, at the beginning of the decay phase, by a dry air intrusion that does not reach the lowest levels of the troposphere. Dry air intrusions have been recognized as common processes in Mediterranean cyclones by Flaounas et al. (2015) but their role in the cyclone lifecycle was not clearly assessed. Here, we suggest that they can act at limiting the extent of the convection at the beginning of the mature phase. The convective activity is stronger during the development than during the mature phase of the cyclone, resulting in heavy rainfall 12 to 6 h before the maximum wind speed, in consistency with previous studies of medicanes based on observations (Miglietta et al., 2013; Dafis et al., 2018). Finally, these results are consistent with those of Carrió et al. (2017). By using a factor separation technique, they show that while the role of the upper-level PV anomaly is crucial in preconditioning the event, its rapid deepening is due to the synergy of latent heat release and upper-level dynamics.

Coupling the atmospheric model with a 3D high-resolution oceanic model shows that the surface cooling susceptible to affect the surface fluxes is too weak in that case to impact the atmospheric destabilization processes at low level. Nevertheless, the effect of the medicane on the oceanic surface layer is probably significant. To better understand the sea surface evolution and the role of coupling, the ocean mixed layer response to the medicane and the mechanisms involved will be investigated in more details in future work.

Author contributions. MNB and CLB designed the simulations. MNB performed the simulations. Both authors interpreted the results and wrote the paper.

Competing interests. The author declare that they have no conflict of interest.

Acknowledgments

This work is a contribution to the HyMeX program (Hydrological cycle in the Mediterranean EXperiment - <http://www.hymex.org>) through INSU-MISTRALS support. The authors acknowledge the Pôle de Calcul et de Données Marines for the DATARMOR facilities (storage, data access, computational resources). The authors acknowledge the MISTRALS/HyMeX database teams (ESPRI/IPSL and SEDOO/OMP) for their help in accessing to the surface weather station data. The PSY2V4R4 daily analyses were made available by the Copernicus Marine Environment Monitoring Service (<http://marine.copernicus.eu>). The ERA5 reanalysis at hourly timescales (doi: 10.24381/cds.bd0915c6) are produced by the European Centre for Medium-Range Weather Forecasts (ECMWF) and made available by the Copernicus Climate Change Service (<https://cds.climate.copernicus.eu>). METAR observations of SLP and wind were retrieved through the Weather Wunderground portal <https://www.wunderground.com>. The authors thank J.-L. Redelsperger (LOPS) for valuable discussions. We also thank E. Flaounas and an anonymous reviewer whose comments helped to greatly improve this paper.

References

- Akhtar, N., Brauch, J., Dobler, A., Béranger, K. and Ahrens, B.: Medicanes in an ocean–atmosphere coupled regional climate model, *Nat. Hazards Earth Syst. Sci*, 14, 2189–2201, 2014.
- Arsouze, T., Beuvier, J., Béranger, K., Somot, S., Lebeaupin Brossier, C., Bourdallé-Badie, R., Sevault, F., and Drillet, Y.: Sensibility analysis of the Western Mediterranean Transition inferred by four companion simulations, The Mediterranean Science Commission, Monaco, in *Proceedings of the 40th CIESM Congress*, November 2013, Marseille, France, 2013.
- Barnier, B., Madec, G., Penduff, T., Molines, J.-M., Treguier, A.-M., Le Sommer, J., Beckmann, A., Biastoch, A., Böning, C., Dengg, J., Derval, C., Durand, E., Gulev, S., Remy, E., Talandier, C., Theetten, S., Maltrud, M., McClean, J., and De Cuevas, B.: Impact of partial steps and momentum advection schemes in a global ocean circulation model at eddy-permitting resolution. *Ocean Dyn.* 56 (5), 543–567, <https://doi.org/10.1007/s10236-006-0082-1>, 2006.
- Belamari, S.: Report on uncertainty estimates of an optimal bulk formulation for surface turbulent fluxes, Marine EnviRonment and Security for the European Area–Integrated Project (MERSEA IP), Deliverable D, 4, 2005.
- Belamari, S. and Pirani, A.: Validation of the optimal heat and momentum fluxes using the ORCA2-LIM global ocean-ice model, Marine EnviRonment and Security for the European Area–Integrated Project (MERSEA IP), Deliverable D, 4, 2007.

- Beuvier, J., Béranger, K., Lebeaupin Brossier, C., Somot, S., Sevault, F., Drillet, Y., Bourdallé-Badie, R., Ferry, N., and Lyard, F.: Spreading of the Western Mediterranean deep water after winter 2005: time scales and deep cyclone transport, *J. Geophys. Res.: Oceans* 117 (C7), <https://doi.org/10.1029/2011JC007679>. C07022, 2012.
- Black, W. J., and Dickey, T.D.: Observations and analyses of upper ocean responses to tropical storms and hurricanes in the vicinity of Bermuda, *J. Geophys. Res.*, 113, C08009, doi:10.1029/2007JC004358, 2008.
- Blanke, B., and Delecluse, P.: Variability of the tropical Atlantic Ocean simulated by a general circulation model with two different mixed-layer physics. *J. Phys. Oceanogr.* 23 (7), 1363–1388. <https://doi.org/10.1175/1520-0485023<1363:VOTTAO>2.0.CO;2>, 1993.
- Bougeault, P. and Lacarrère, P.: Parameterization of Orography-Induced Turbulence in a Mesobeta-Scale Model. *Mon. Weather Rev.*, 117, 1872–1890. [https://doi.org/10.1175/1520-0493\(1989\)117<1872:POOITI>2.0.CO;2](https://doi.org/10.1175/1520-0493(1989)117<1872:POOITI>2.0.CO;2), 1989.
- Bresson, E., Ducrocq, V., Nuissier, O., Ricard, D., and de Saint-Aubin, C.: Idealized numerical study of southern France heavy precipitating events: Identification of favouring ingredients. *Q. J. R. Meteorol. Soc.*, 138: 1751–1763, 2012.
- Carrió, D. S., Homar, V., Jansà, A., Romero, R. and Picornell, M. A.: Tropicalization process of the 7 November 2014 Mediterranean cyclone: numerical sensitivity study, *Atmospheric Research*, 197, 300–312, 2017.
- Chaboureau, J.-P., Pantillon, F., Lambert, D., Richard, E. and Claud, C.: Tropical transition of a Mediterranean storm by jet crossing, *Q. J. Roy. Meteorol. Soc.*, 138, 596–611, 2012.
- Cioni, G., Cerrai D., and Klocke D.: Investigating the predictability of a Mediterranean tropical-like cyclone using a storm-resolving model, *Q. J. Roy. Met. Soc.*, 144, 1598–1610, doi: 10.1102/qj.3322, 2018.
- Colella, P. and Woodward, P.R.: The Piecewise Parabolic Method (PPM) for Gas-Dynamical Simulations. *Journal of Computational Physics*, 54, 174–201, [https://doi.org/10.1016/0021-9991\(84\)90143-8](https://doi.org/10.1016/0021-9991(84)90143-8), 1984.
- Cuxart, J., Bougeault, P. and Redelsperger, J.L.: A turbulence scheme allowing for mesoscale and large-eddy simulations, *Q. J. Roy. Meteorol. Soc.*, 126, 1–30. <https://doi.org/10.1002/qj.49712656202>, 2000.
- D'Asaro, E. A., Sanford, T. B., Niiler, P. P., and Terrill, E.J.: Cold wake of Hurricane Frances. *Geophys. Res. Lett.*, 34, L15609, doi:10.1029/2007GL030160, 2007.
- Dafis, S., Rysman, J. F., Claud, C., and Flaounas, E.: Remote sensing of deep convection within a tropical-like cyclone over the Mediterranean Sea. *Atmospheric Science Letters*, 19(6), e823, 2018.
- Di Muzio, E., Riemer, M., Fink, A. H., and Maier-Gerber, M.: Assessing the predictability of Medicanes in ECMWF ensemble forecasts using an object-based approach. *Q. J. R. Meteorol. Soc.*, 145(720), 1202–1217, 2019.
- Ducrocq, V., Nuissier, O., and Ricard, D.: A numerical study of three catastrophic precipitating events over southern France. Part II: Mesoscale triggering and stationarity factors. *Q. J. R. Meteorol. Soc.* 134: 131–145, doi.org/10.1002/qj.199, 2008.
- Emanuel, K.A.: An air–sea interaction theory for tropical cyclones. Part I: Steady-state maintenance, *J. Atmos. Sci.*, 43, 585–604, 1986.
- Fita, L., and Flaounas, E.: Medicanes as subtropical cyclones: the December 2005 case from the perspective of surface pressure tendency diagnostics and atmospheric water budget, *Q. J. Roy. Meteorol. Soc.*, 144, 1028–1044, doi: 10.1002/qj.3273, 2018.
- Flaounas, E., Raveh-Rubin, S., Wernli, H., Drobinski, P. and Bastin, S.: The dynamical structure of intense Mediterranean cyclones, *Clim. Dynam.*, 44, 2411–2427, doi: 10.1007/s00382-014-2330-2, 2015.

- Flaounas, E., et al.: Assessment of an ensemble of ocean–atmosphere coupled and uncoupled regional climate models to reproduce the climatology of Mediterranean cyclones. *Clim. Dynam.*, 51(3), 1023–1040, 2018
- Gaertner, M.A., Gonzalez-Aleman, J.J., Romera, R., Dominguez, M., Gil, V., Sanchez, E., Gallardo, C., Miglietta, M.M., Walsh, K., Sein, D., Somot, S., dell’Aquila, A., Teichmann, C., Ahrens, B., Buonomo, E., Colette, A., Bastin, S., van Meijgaard, E. and Nikulin, G.: Simulation of medicanes over the Mediterranean Sea in a regional climate model ensemble: impact of ocean-atmosphere coupling and increased resolution, *Clim. Dynam.*, 51, 1041–1057, 2017.
- Gheusi, F., and Stein, J.: Lagrangian trajectory and air-mass tracking analyses with Meso-NH by means of Eulerian passive tracers, *Techn. Doc.*, http://mesonh.aero.obs-mip.fr/mesonh/dir_doc/lag_m46_22avril2005/lagrangian46.pdf, accessed on 18/02/2019, 2005.
- Hart, R.E.: A cyclone phase space derived from thermal wind and thermal asymmetry, *Mon. Weather Rev.*, 131, 585–616, 2003.
- Homar, V., Romero, R., Stensrud, D.J., Ramis, C. and Alonso, S.: Numerical diagnosis of a small, quasi-tropical cyclone over the western Mediterranean: dynamical vs. boundary factors, *Q. J. Roy. Meteorol. Soc.*, 129, 1469–1490, 2003.
- Lac, C., Chaboureaud, J.-P., Masson, V., et al.: Overview of the Meso-NH model version 5.4 and its applications, *Geosci. Model Dev.*, 1, 1929–1969, <https://doi.org/10.5194/gmd-11-1929-2018>, 2018.
- Lazar, A., Madec, G., and Delecluse, P.: The deep interior downwelling, the Veronis effect, and mesoscale tracer transport parameterizations in an OGCM. *J. Phys. Oceanogr.* 29 (11), 2945–2961. [https://doi.org/10.1175/1520-0485\(1999\)029<2945:TDIDTV>2.0.CO;2](https://doi.org/10.1175/1520-0485(1999)029<2945:TDIDTV>2.0.CO;2), 1999.
- Lebeaupin Brossier, C., Arsouze, T., Béranger, K., Bouin, M.-N., Bresson, E., Ducrocq, V., Giordani, H., Nuret, M., Rainaud, R., and Taupier-Letage, I.: Ocean Mixed Layer responses to intense meteorological events during HyMeX-SOP1 from a high-resolution ocean simulation, *Ocean Model.*, 84, 84–103. <https://doi.org/10.1016/j.ocemod.2014.09.009>, 2014.
- Lellouche, J.-M., Le Galloudec, O., Drévillon, M., Régnier, C., Greiner, E., Garric, G., Ferry, N., Desportes, C., Testut, C.-E., Bricaud, C., Bourdallé-Badie, R., Tranchant, B., Benkiran, M., Drillet, Y., Daudin, A., and De Nicola, C.: Evaluation of global monitoring and forecasting systems at Mercator Océan, *Ocean Sci.*, 9, 57–81, <https://doi.org/10.5194/os-9-57-2013>, 2013.
- Liu, W. T., Katsaros, K. B., and Businger, J. A: Bulk parameterization of air-sea exchanges of heat and water vapor including the molecular constraints at the interface, *J. Atmos. Sci.*, 36, 1722–1735, 1979.
- Lyard, F., Lefevre, F., Letellier, T., and Francis, O.: Modelling the global ocean tides: modern insights from FES2004. *Ocean Dyn.*, 56 (5), 394–415. <https://doi.org/10.1007/s10236-006-0086-x>, 2006.
- Madec, G., and Imbard, M.: A global ocean mesh to overcome the north pole singularity. *Clim. Dyn.*, 12, 381–388, 1996.
- Madec, G., and the NEMO Team: NEMO ocean engine. Note du Pole de modélisation, Institut Pierre-Simon Laplace (IPSL), France, ISSN No 1288–1619. 27, 2016.
- Masson, V., Le Moigne, P., Martin, E., Faroux, S., Alias, A., Alkama, R., Belamari, S., Barbu, A., Boone, A., Bouysse, F., Brousseau, P., Brun, E., Calvet, J.C., Carrer, D., Decharme, B., Delire, C., Donier, S., Essaouini, K., Gibelin, A.L., Giordani, H., Habets, F., Jidane, M., Kerdraon, G., Kourzeneva, E., Lafaysse, M., Lafont, S., Lebeaupin-Brossier, C., Lemsu, A., Mahfouf, J.-F., Marguinaud, P., Mokhtari, M., Morin, S., Pigeon, G., Salgado, R., Seity, Y., Taillefer, F., Tanguy, G., Tulet, P., Vincendon, B., Vionnet, V. and Voldoire, A.: The SURFEXv7.2 land and ocean surface platform for coupled or offline simulation of Earth surface variables and fluxes, *Geosci. Model Dev.*, 6, 929–960, <https://doi.org/10.5194/gmd-6-929-2013>, 2013.

- McTaggart-Cowan, R., Davies, E. L., Fairman Jr, J. G., Galarneau Jr, T. J., and Schultz, D. M.: Revisiting the 26.5 C sea surface temperature threshold for tropical cyclone development. *Bull. American Meteorol. Soc.*, 96(11), 1929-1943, 2015.
- Mesinger, F. and Arakawa, A.: Numerical Methods Used In Atmospheric Models, Global Atmospheric Research Program Publication Series 17(1), 1976
- Miglietta, M. M., Moscatello, A., Conte, D., Mannarini, G., Lacorata, G., and Rotunno, R: Numerical analysis of a Mediterranean “hurricane” over south-eastern Italy: Sensitivity experiments to sea surface temperature, *Atmos. Res.*, 101, 412–426, 2011.
- Miglietta, M.M., Laviola, S., Malvaldi, A., Conte, D., Levizzani, V. and Price, C.: Analysis of tropical-like cyclones over the Mediterranean Sea through a combined modelling and satellite approach, *Geophys. Res. Lett.*, 40, 2400–2405, 2013.
- Miglietta, M.M., Cerrai, D., Laviola, S., Cattani, E. and Levizzani, V.: Potential vorticity patterns in Mediterranean “hurricanes”. *Geophys. Res. Lett.*, 44, 2537–2545, 2017.
- Miglietta, M.M., and Rotunno, R.: Development mechanisms for Mediterranean tropical-like cyclones (medicanes), *Q. J. Roy. Meteorol. Soc.*, 1–17. <https://doi.org/10.1002/qj.3503>, 2019.
- Morcrette, J.-J.: Radiation and cloud radiative properties in the ECMWF operational weather forecast model. *J. Geophys. Res.*, 96D, 9121-9132, 1991.
- Moscatello, A., Miglietta, M.M. and Rotunno, R.: Numerical analysis of a Mediterranean “hurricane” over southeastern Italy, *Mon. Weather Rev.*, 136, 4373–4397, 2008.
- Myers, J. L., Well, A. D., and Lorch, R.F. Jr: Research Design and Statistical Analysis (3rd ed.), Taylor and Francis Eds., New York, 2010.
- Noyelle, R., Ulbrich, U., Becker, N., and Meredith, E. P.: Assessing the impact of sea surface temperatures on a simulated medicanes using ensemble simulations, *Nat. Hazards Earth Syst. Sci.*, 19, 941–955, <https://doi.org/10.5194/nhess-19-941-2019>, 2019.
- Pergaud, J., Masson, V., Malardel, S. and Couvreux, F.: A parameterization of dry thermals and shallow cumuli for mesoscale numerical weather prediction, *Bound.-Layer. Meteor.*, 132, 83-106, doi: 10.1007/s10546-009-9388-0, 2009.
- Picornell, M. A., Campins, J., and Jansà, A.: Detection and thermal description of medicanes from numerical simulation, *Nat. Hazards Earth Syst. Sci.*, 14, 1059–1070, 2014.
- Pytharoulis, I.: Analysis of a Mediterranean tropical-like cyclone and its sensitivity to the sea surface temperatures. *Atmospheric Research*, 208, 167–179, 2018.
- Rainaud, R., Lebeaupin Brossier, C., Ducrocq, V., and Giordani, H.: High-resolution air-sea coupling impact on two heavy precipitation events in the Western Mediterranean. *Quart. J. Roy. Meteor. Soc.*, 143, 2448–2462, <https://doi.org/10.1002/qj.3098>, 2017.
- Reale, O. and Atlas, R.: Tropical cyclone-like vortices in the extratropics: observational evidence and synoptic analysis. *Weather and Forecasting*, 16, 7–34, 2001.
- Redelsperger, J.L. and Sommeria, G.: Three-dimensional simulation of a convective storm: Sensitivity studies on subgrid parameterization and spatial resolution, *J. Atmos. Sci.*, 43, 2619–2635, [https://doi.org/10.1175/1520-0469\(1986\)043<2619:TDSOAC.2.0.CO;2](https://doi.org/10.1175/1520-0469(1986)043<2619:TDSOAC.2.0.CO;2), 1986.
- Redelsperger, J.-L., Mahé, F. and Carlotti, P.: A simple and general subgrid model suitable both for surface layer and free-stream turbulence. *Bound.-Layer. Meteor.*, 101, 375–408. <https://doi.org/10.1023/A:1019206001292>, 2001.

- Reed, R.J., Kuo, Y.-H., Albright, M.D., Gao, K., Guo, Y.-R. and Huang, W.: Analysis and modeling of a tropical-like cyclone in the Mediterranean Sea, *Meteorol. Atmos. Phys.*, 76, 183–202, 2001.
- Renault, L., Chiggiato, J., Warner, J.C., Gomez, M., Vizoso, G. and Tintoré, J.: Coupled atmosphere-ocean-wave simulations of a storm event over the Gulf of Lion and Balearic Sea, *J. Geophys. Res.*, 117, C09019, doi:10.1029/2012JC007924, 2012.
- Ricchi, A., Miglietta, M.M., Barbariol, F., Benetazzo, A., Bergamasco, A., Bonaldo, D., Cassardo, C., Falcieri, F.M., Modugno, G., Russo, A., Sclavo, M. and Carniel, S.: Sensitivity of a Mediterranean tropical-like cyclone to different model configurations and coupling strategies, *Atmosphere*, 8(5), 92, 1–32, <https://doi.org/10.3390/atmos8050092>, 2017.
- Rotunno, R. and Emanuel, K.: An air–sea interaction theory for tropical cyclones. Part II: Evolutionary study using a nonhydrostatic axisymmetric numerical model. *J. Atmos. Sci.*, 44, 542–561, 1987.
- Roullet, G., and Madec, G.: Salt conservation, free surface and varying levels: a new formulation for ocean general circulation models. *J. Geophys. Res.* 105 (C10), 23927–23942. <https://doi.org/10.1029/2000JC900089>, 2000.
- Schade, L. R., and Emanuel, K. A.: The ocean’s effect on the intensity of tropical cyclones: Results from a simple coupled atmosphere–ocean model. *J. Atmos. Sci.*, 56, 642–651, 1999.
- Schär, C., and Wernli, H.: Structure and evolution of an isolated semi-geostrophic cyclone. *Q. J. R. Meteorol. Soc.*, 119(509), 57–90, 1993.
- Seity, Y., Brousseau, P., Malardel, S., Hello, G., Bénard, P., Bouttier, F., Lac, D. and Masson, V.: The AROME-France convective-scale operational model. *Mon. Weather Rev.*, 139, 976–991. <https://doi.org/10.1175/2010MWR3425.1>, 2011.
- Tibaldi, S., Buzzi, A. and Speranza, A.: Orographic cyclogenesis, in *Extratropical cyclones, The Palmen Memorial volume*, edited by: Newton, C., and Holopainen, E. O. American Meteorological Society, Boston, 107–127, 1990.
- Tous, M. and Romero, R.: Meteorological environments associated with medicane development, *Int. J. Climatol.*, 33, 1–14, 2013.
- Trenberth, K.: Uncertainty in hurricanes and global warming, *Science*, 308 (5729), 1753–1754, doi:10.1126/science.1112551, 2005.
- Voldoire, A., Decharme, B., Pianezze, J., Lebeaupin Brossier, C., Sevault, F., Seyfried, L., Garnier, V., Bielli, S., Valcke, S., Alias, A., Accensi, M., Arduin, F., Bouin, M.-N., Ducrocq, V., Faroux, S., Giordani, H., Léger, F., Marsaleix, P., Rainaud, R., Redelsperger, J.-L., Richard, E., and Riette, S.: SURFEX v8.0 interface with OASIS3-MCT to couple atmosphere with hydrology, ocean, waves and sea-ice models, from coastal to global scales, *Geosci. Model Dev.*, 10, 4207–4227, <https://doi.org/10.5194/gmd-10-4207-2017>, 2017.

Tables

	U_{10}	θ	SST	q
$H+LE$	0.66	-0.20	0.35	0.48
LE	0.65	0.10	0.36	0.33
H	0.38	-0.70	0.21	
U_{10}		-0.10	-0.25	0.84
θ			-0.04	-0.03
SST				-0.18

Table 1: Spearman's rank correlations between the enthalpy flux, latent and sensible heat flux and related parameters (10 m wind speed U_{10} , potential temperature at 10 m θ , SST and humidity at 10 m q) at 09:00 UTC on 7 November, from the CPL simulation, on the EF600 area.

	U_{10}	θ	SST	q
$H+LE$	0.62	-0.14	0.28	0.49
LE	0.49	0.22	0.42	0.23
H	0.55	-0.72	-0.10	
U_{10}		-0.19	-0.38	0.87
θ			0.41	-0.32
SST				-0.34

Table 2: Same at Table 1 at 13:00 UTC on 7 November.

	U_{10}	θ	SST	q
$H+LE$	0.31	-0.09	0.32	0.17
LE	0.16	0.26	0.46	-0.03
H	0.37	-0.75	-0.20	
U_{10}		-0.02	-0.52	0.93
θ			0.40	-0.04
SST				-0.49

Table 3: Same at Table 1 at 18:00 UTC on 7 November.

Figures

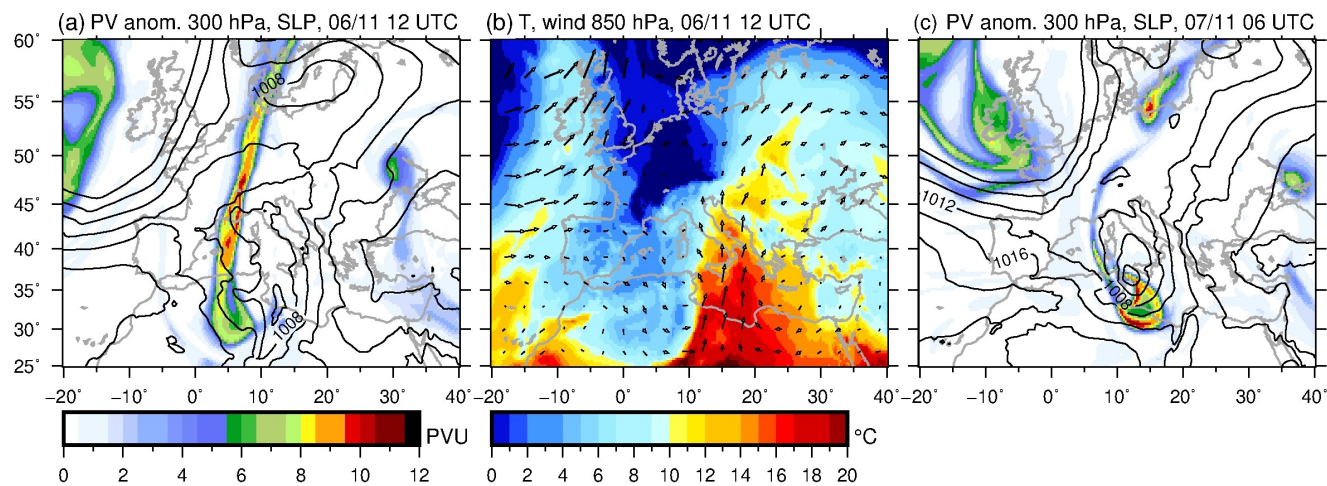


Figure 1: Potential vorticity (PV) anomaly at 300 hPa (colour scale) and SLP (isocontours every 4 hPa) at 12:00 UTC on 6 November (a) and 06:00 UTC on 7 November (c), temperature (colour scale, °C) and wind at 850 hPa at 06:00 UTC on 6 November (b) from the ERA5 reanalysis.

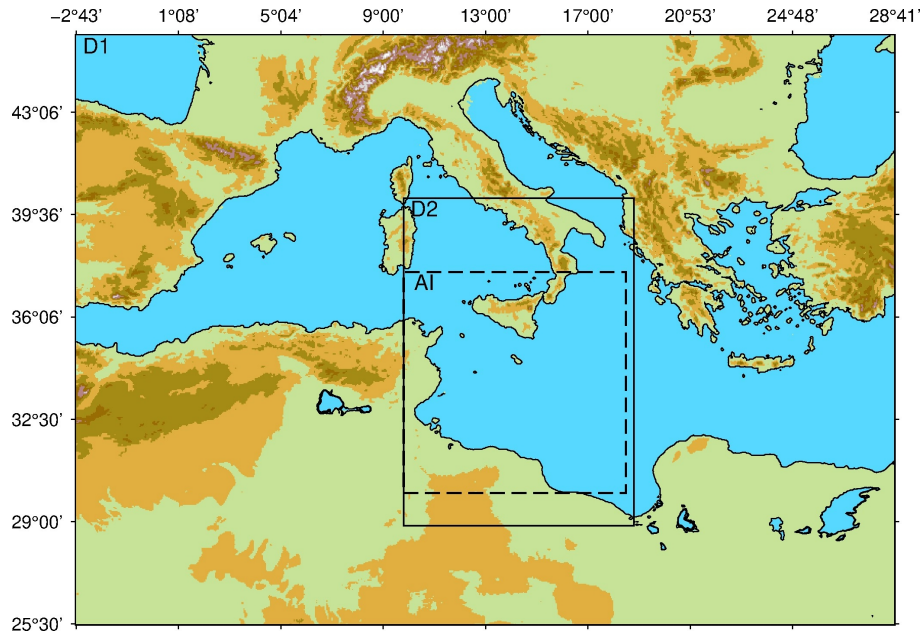


Figure 2: Map of the large-scale domain D1, with the domain D2 indicated by the solid-line frame and the area of interest (AI) indicated by the dashed-line frame.

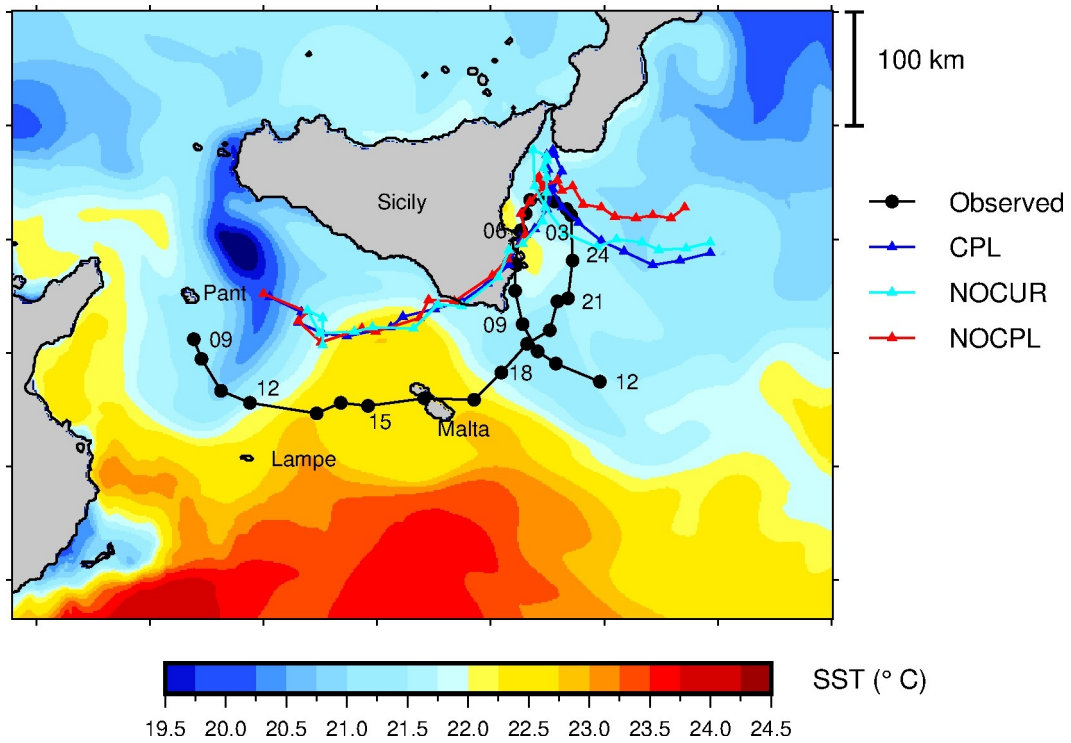


Figure 3: Comparison of the simulated tracks (triangles) of the non-coupled run (NOCPL, red), coupled run with SST only (NOCUR, cyan) and fully coupled run (CPL, blue) with the best track (black closed circles) based on observations as in Cioni et al., (2018). The position is shown every hour with time labels every 3 h, starting at 09:00 UTC on 7 November until 12:00 UTC on 8 November. In colours, initial Sea Surface Temperature (SST, $^{\circ}\text{C}$) at 01:00 UTC on 7 November.

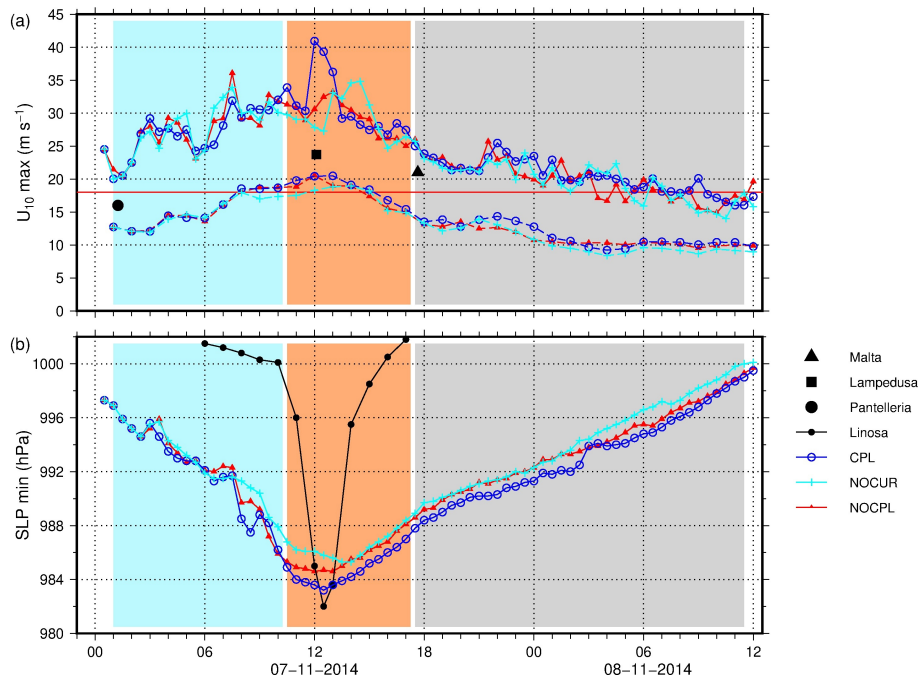


Figure 4: Time series of the maximum of the 10 m wind speed, and 10 m wind averaged over a 100 km radius around the cyclone centre (a) and minimum sea-level pressure (b) as obtained in the different simulations on the 7 November and 8 November until 12:00 UTC. The thin red line in (a) indicates the 18 m s^{-1} wind speed threshold. The background shading (here and in the following time-series plots) indicates the development (light blue), mature (orange) and decay (grey) phases. The observations of SLP in Linosa (black plain circles) are shown for comparison in (b), the observations of wind speed from Malta, Lampedusa and Pantelleria are shown in (a) – see text.

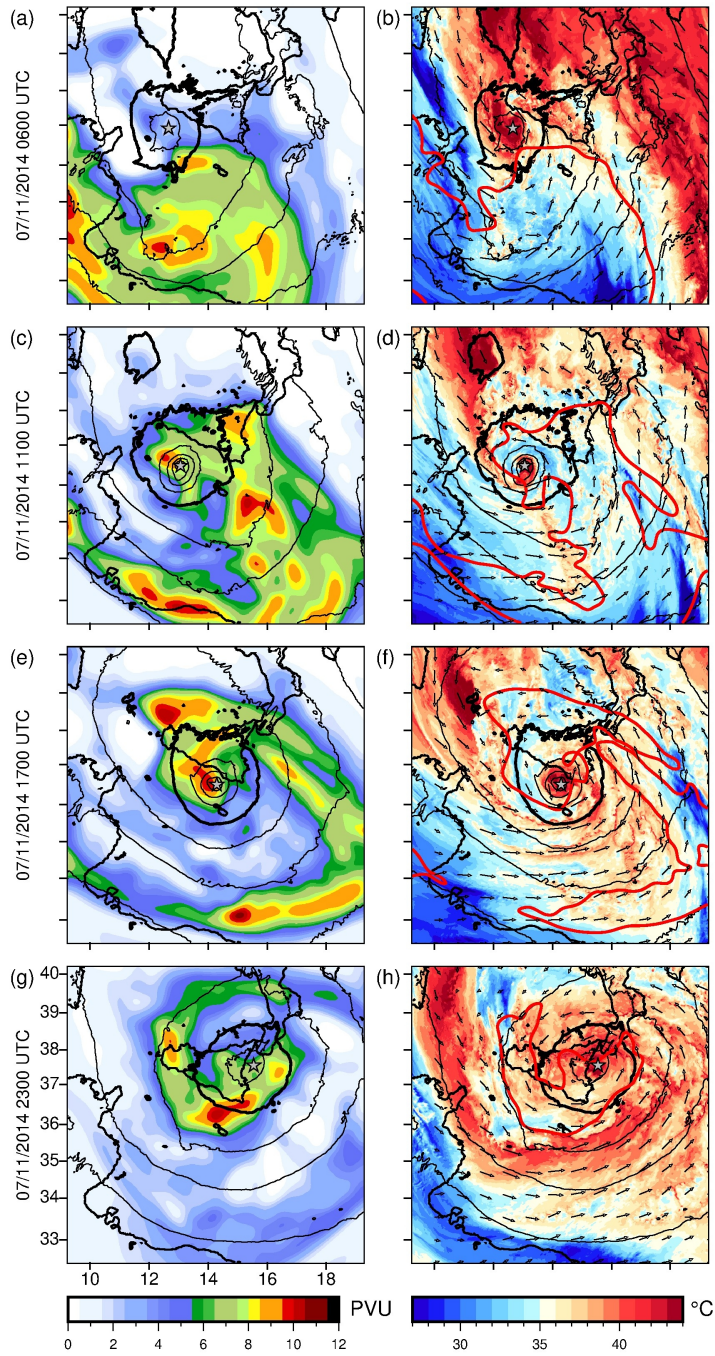


Figure 5: Potential vorticity at 300 hPa (colour scale) and SLP (isocontours every 4 hPa, the 1000 hPa isobar is in bold), (a, c, e, g) and equivalent potential temperature ($^{\circ}\text{C}$, colour scale) and wind at 850 hPa, SLP, and 6 PVU at 300 hPa isocontours (red), (b, d, f, h) from the NOCPL simulation.

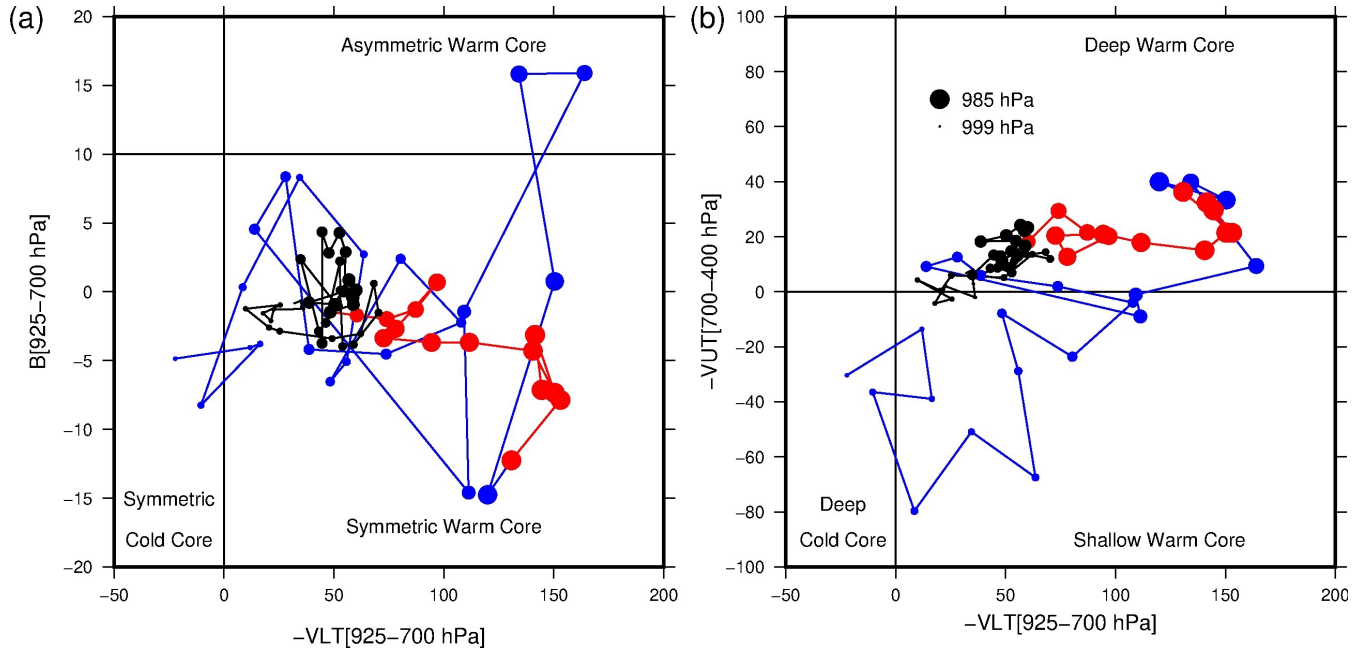


Figure 6: Phase diagram of the NOCPL simulated cyclone from 01:00 UTC on 7 November till 12:00 UTC on 8 November, with low-tropospheric thickness asymmetry inside the cyclone (B) with respect to low-tropospheric thermal wind ($-V_{LT}$) (a), and upper-tropospheric thermal wind ($-V_{UT}$) with respect to low-tropospheric thermal wind (b). The development phase is in blue, the mature phase in red, and the decay phase in black.

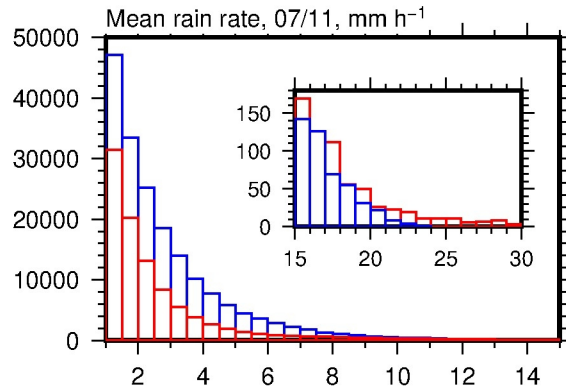


Figure 7: Histogram of the mean rain rate distribution (in number of grid points) for the development (blue) and mature (red) phases in the NOCPL simulation. The enclosed figure shows a zoom on the highest rates.

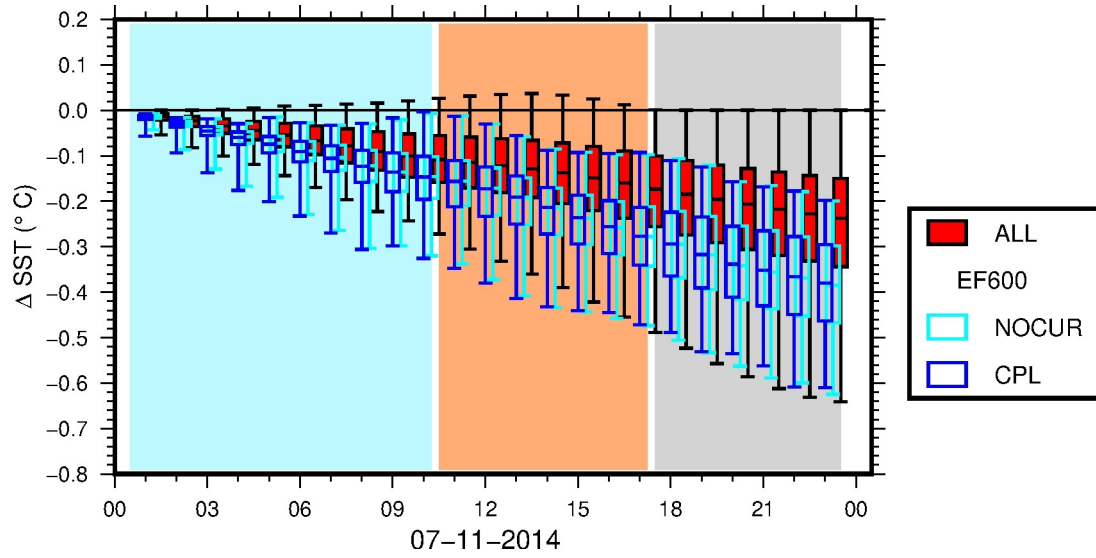


Figure 8: Time series of the median differences between the SST in the CPL and NOCPL simulations, on the whole domain (red) and on the EF600 area (blue, see text for definition), on the 7 November. The boxes indicate the 25 and 75% quantiles and the whiskers the 5 and 95% quantiles. Are also shown the differences between the NOCUR and NOCPL simulations (cyan). Some of the boxes have been slightly shifted horizontally for clarity.

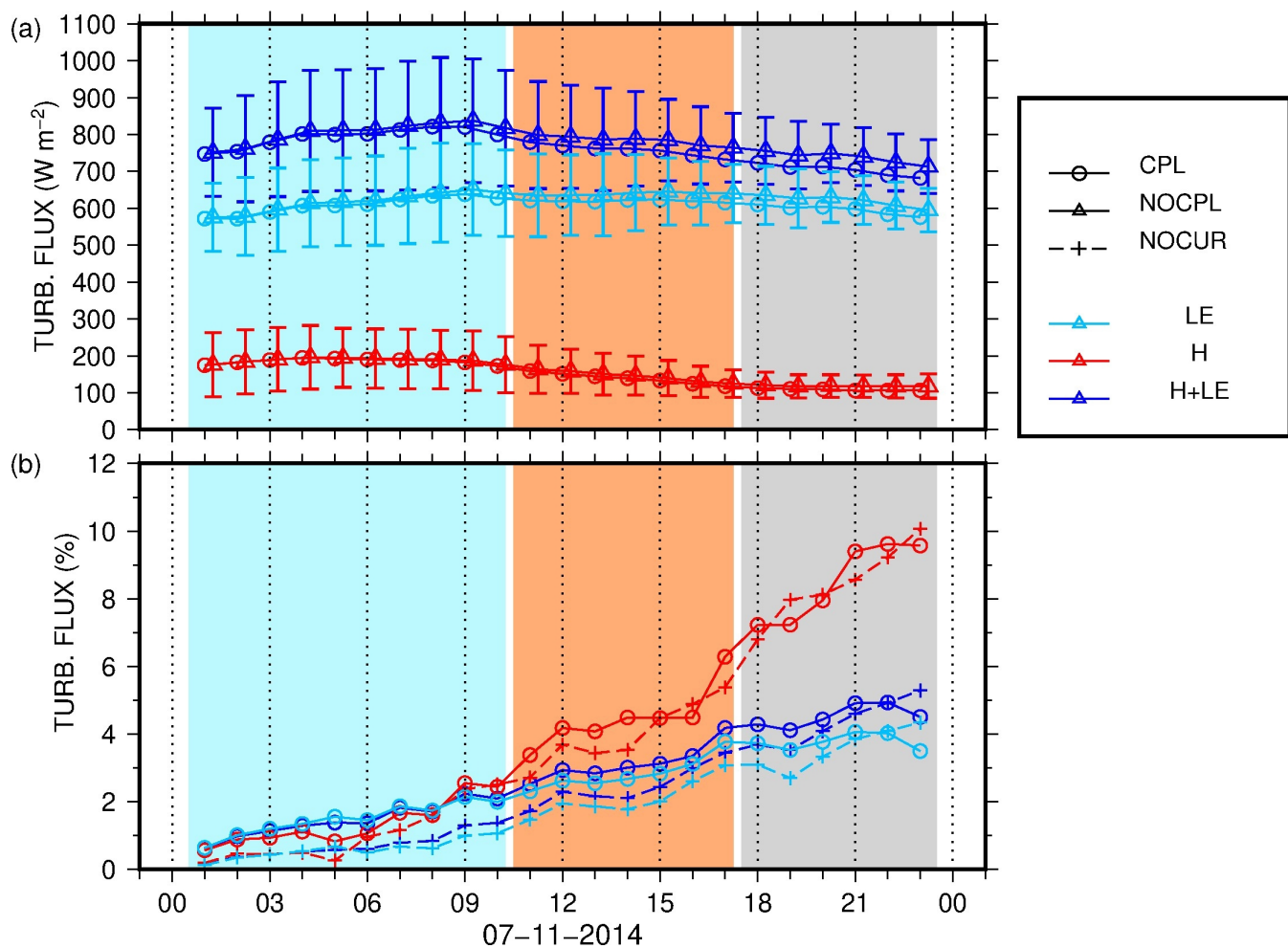


Figure 9: Time series of the mean values and standard deviation (error bars) of the total turbulent heat flux (blue), latent (cyan) and sensible heat flux (red) in the CPL (open circles) and NOCPL (triangles) simulations (a) and of the mean difference between CPL and NOCPL turbulent fluxes (open circles, same colour code) and between NOCUR and NOCPL turbulent fluxes, in percent relative to the NOCPL values (b) on the EF600 area.

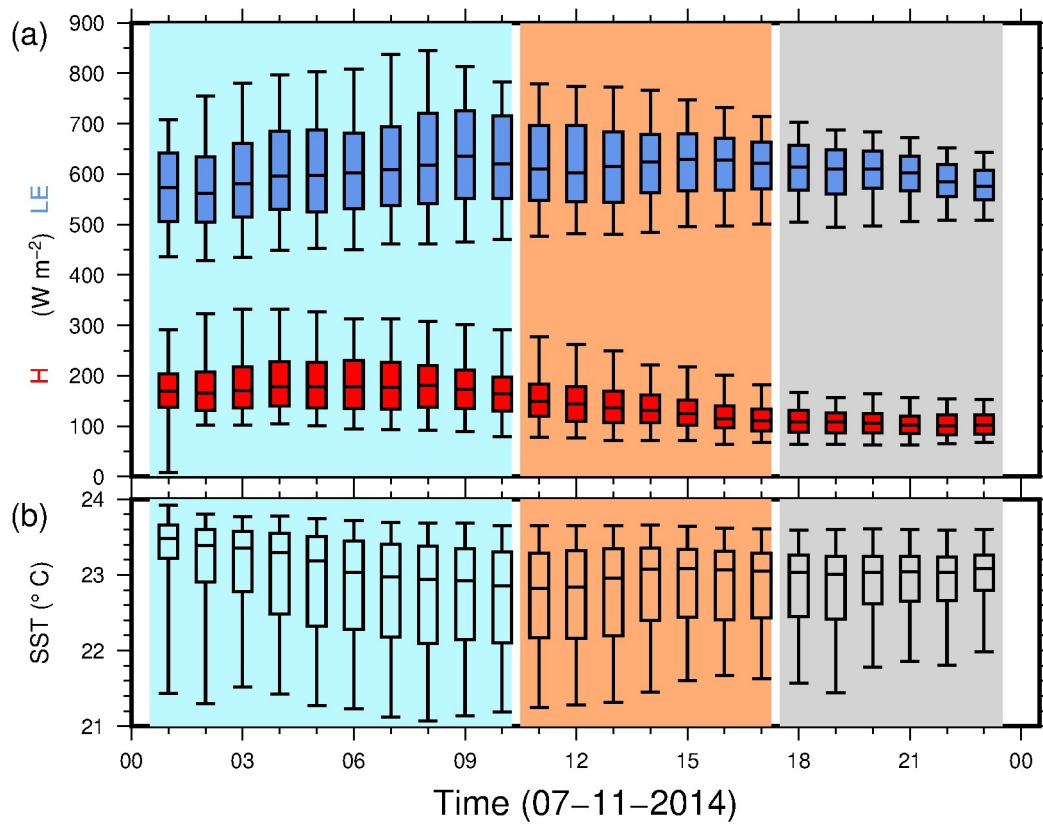


Figure 10: Time series of the median values of latent (blue) and sensible heat fluxes (red, a) and of SST (b) on the EF600 area (see text) on the 7 November. The boxes corresponds to the 25 and 75% quantiles, the whiskers to the 5 and 95% quantiles.

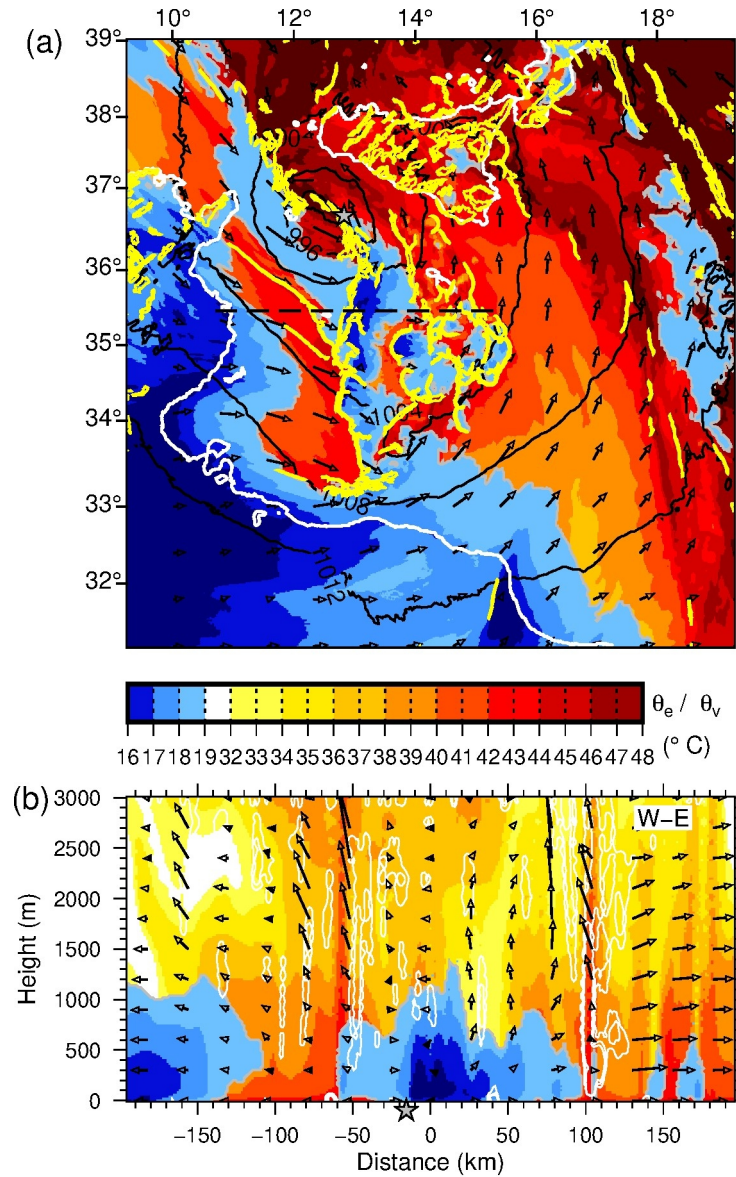


Figure 11: Map of equivalent potential temperature (warm colors) and virtual potential temperature below 19 °C (blue shades), horizontal convergence rate above $1 \times 10^{-3} \text{ m s}^{-2}$ (yellow contours), 10 m wind (arrows) and SLP (black contours) at 08:30 UTC on 7 November (a), and vertical cross-section of equivalent potential temperature and virtual potential temperature (colour scale), tangential wind (black vectors, the vertical component is amplified by a factor 20), potential vorticity anomaly (white contour at 5 PVU) along a west-east transect (b) (dashed line in (a)). The grey stars indicate the position of the SLP minimum.

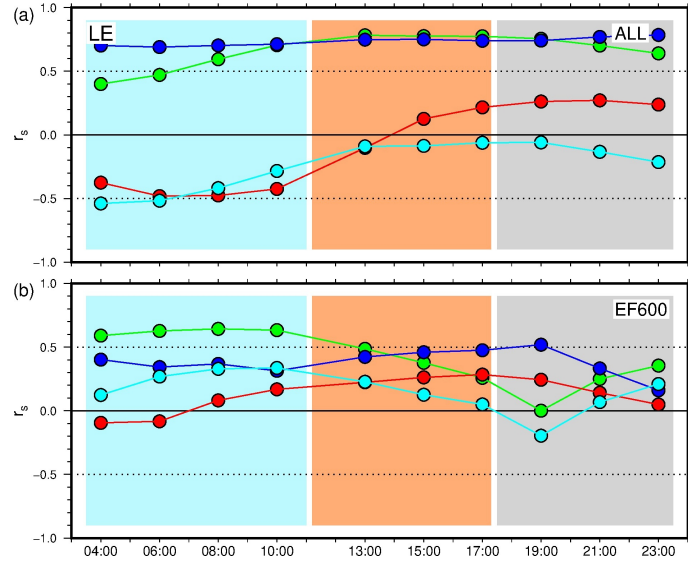


Figure 12: Time series of Spearman's rank-order correlation r_s between the latent heat flux LE and 10 m wind speed (green), potential temperature at 10 m (red), SST (blue) and specific humidity at 2 m (cyan) on the whole domain (a) and EF600 area (b), in the CPL simulation.

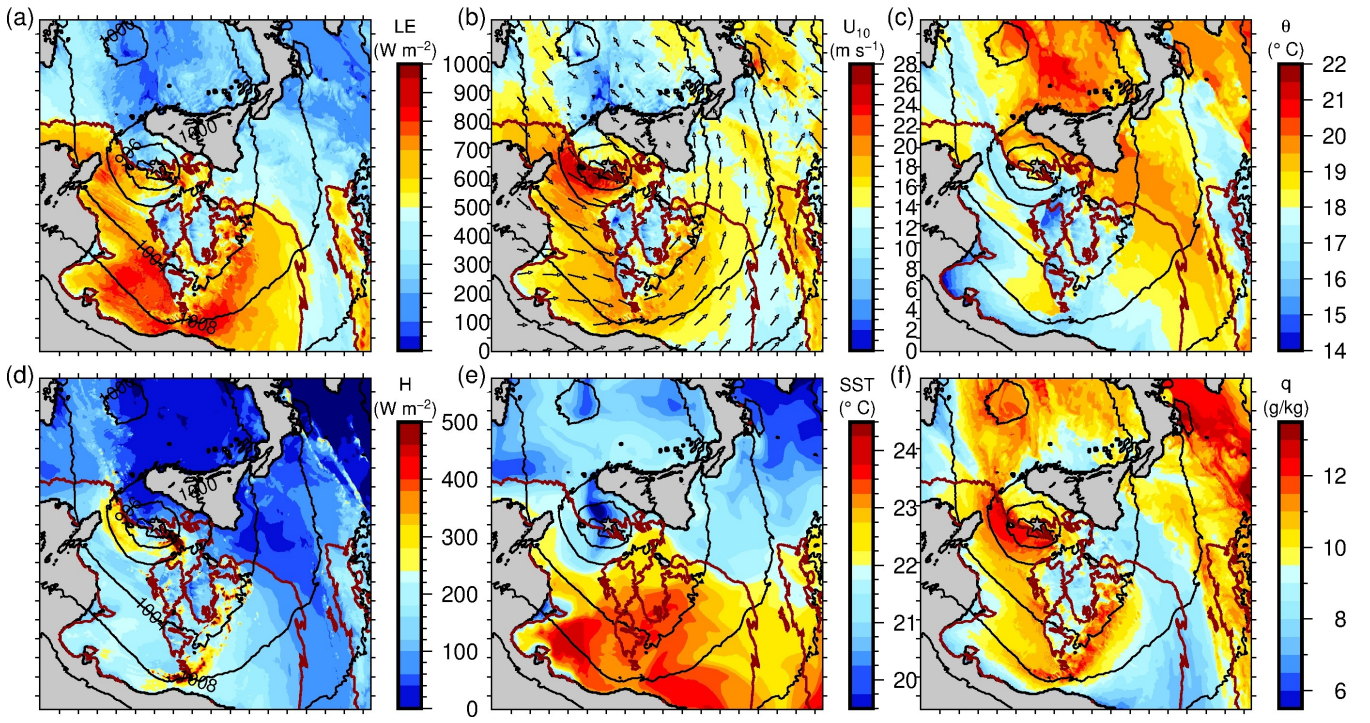


Figure 13: Maps of the total turbulent heat fluxes LE (a), H (b), the 10 m wind U_{10} (c), the 10 m potential temperature (d), the SST (e) and the specific humidity at 2 m (f) at 09:00 UTC on 7 November, in the CPL simulation.

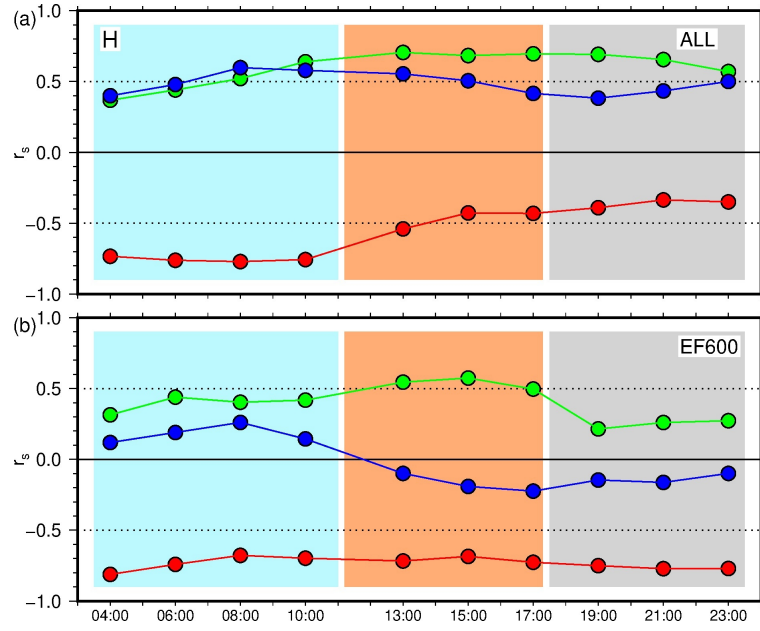


Figure 14: Same as Figure 12 but between the sensible heat flux H and 10 m wind speed (green), potential temperature at 10 m (red), and SST (blue) on the whole domain (a) and EF600 area (b), in the CPL simulation.

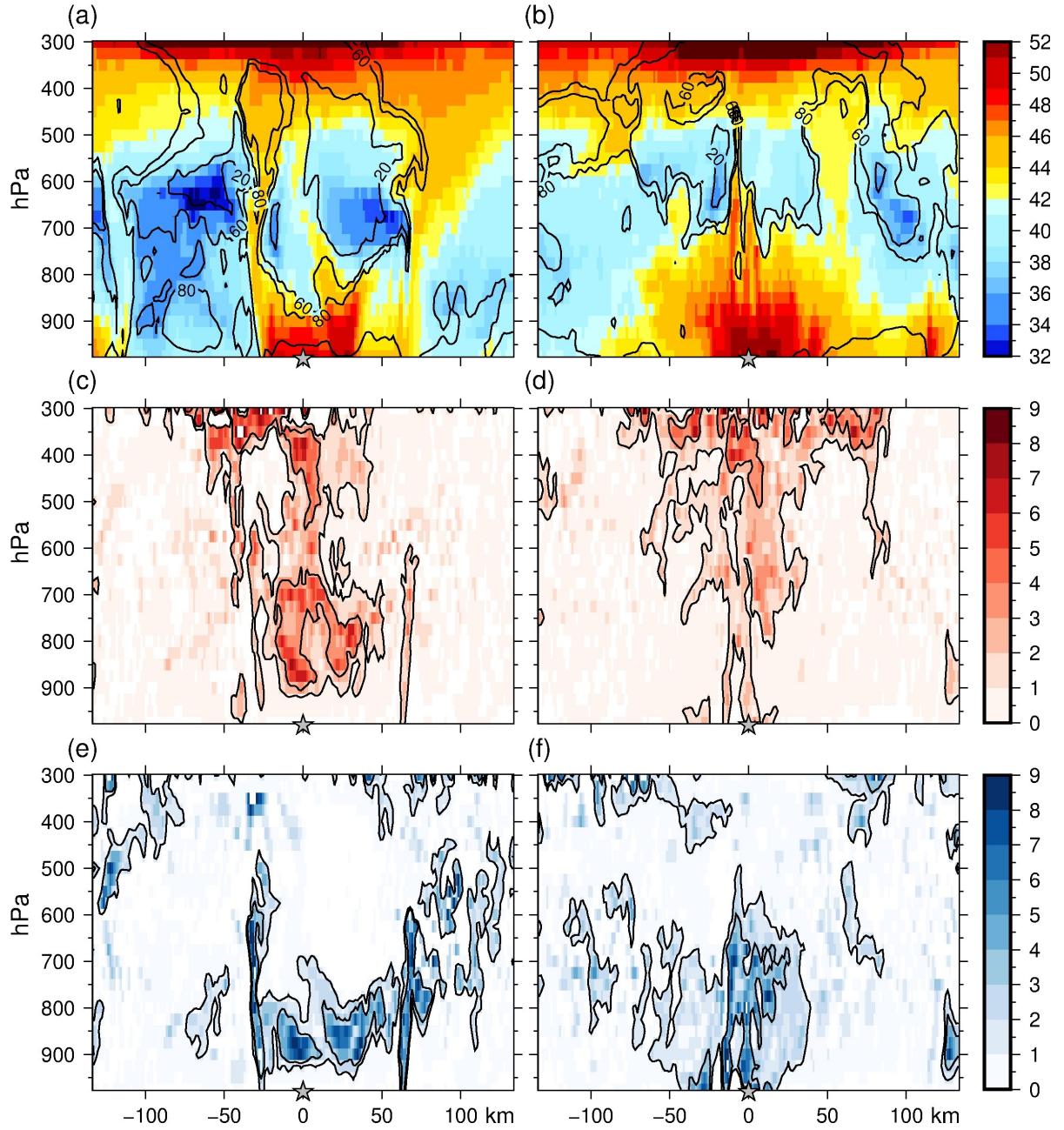


Figure 15: Vertical cross-sections of equivalent potential temperature θ_e (°C, colour scale) and relative humidity (%), (a,b), DPV (intensity), (c,d) and WPV (intensity), (e,f) on a west-east transect across the cyclone centre, at 13:00 (a,c,e) and 18:00 UTC (b,d,f) on 7 November, in the CPL simulation. The black contours in (c) to (f) correspond to intensities 1 and 3 (as defined in Miglietta et al., 2017).

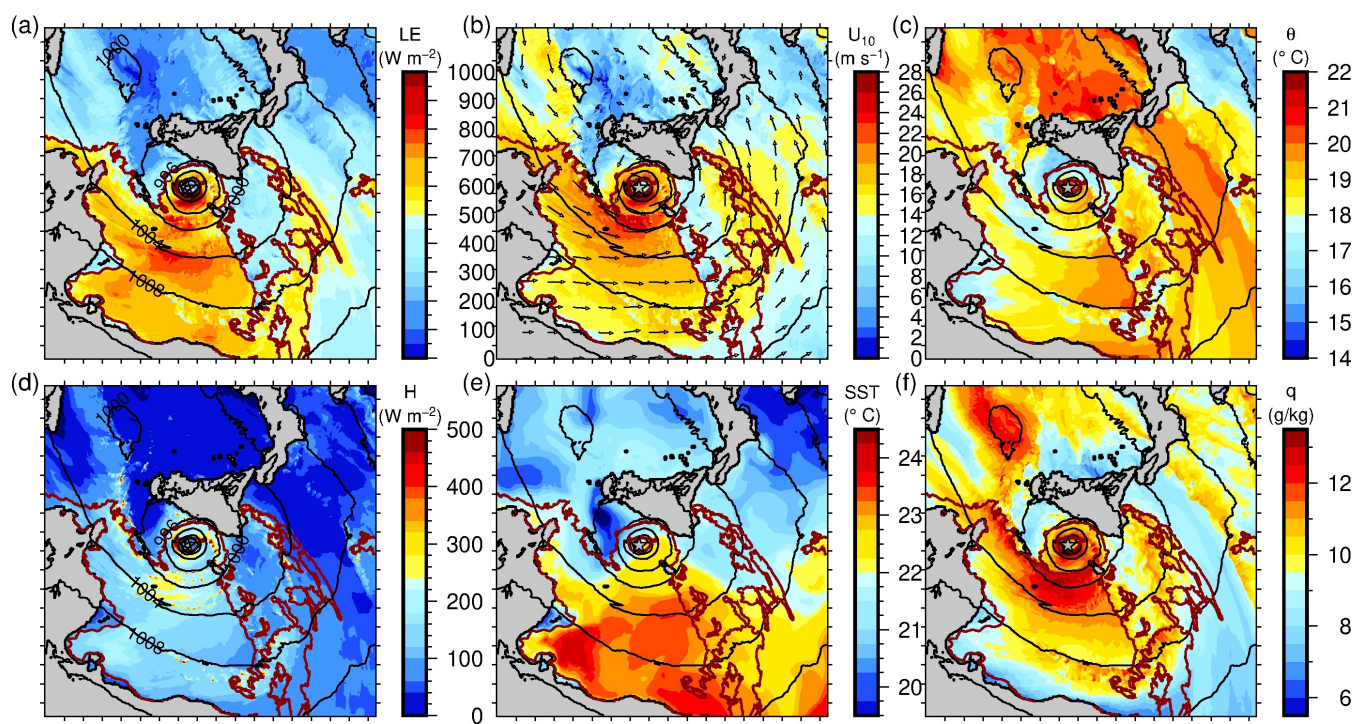


Figure 16: Same as Figure 13 but at 13:00 UTC on 7 November.

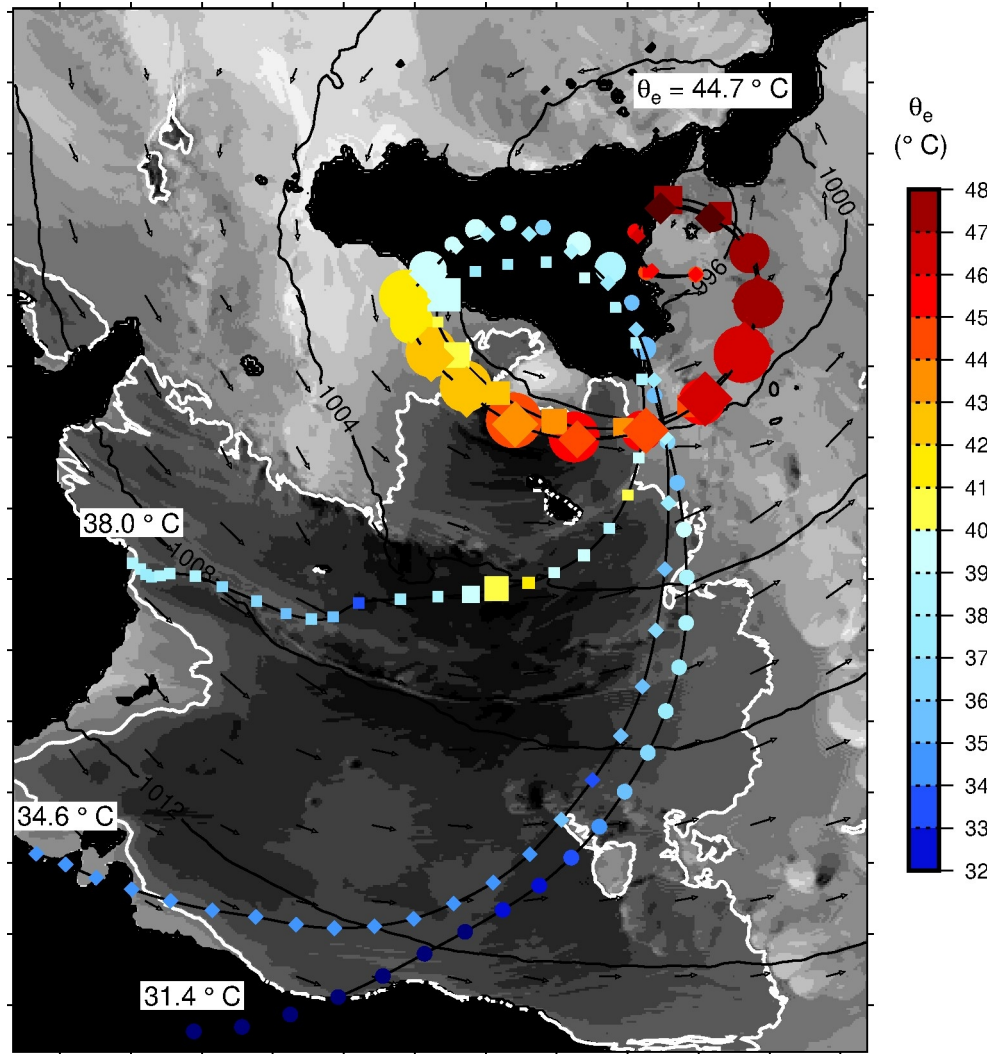


Figure 17: Map of the backtrajectories of air parcels arriving south of the cyclone centre at 23:00 UTC on 7 November, 1500 m above sea level, at 3 different levels (circles, squares and diamonds). The first point of the trajectories correspond to the start of the D2 domain simulation (00 UTC the 07 November). The colour scale indicates the equivalent potential temperature ($^{\circ}\text{C}$) and the size of the symbol is inversely proportional to altitude between 0 and 1000 m. Are also shown the values of the final equivalent potential temperature, of the initial equivalent potential temperatures, the wind field at 900 hPa (black vectors), and the surface enthalpy flux (grey shades) with a threshold at 600 W m^{-2} (white contour) at 15:30 UTC when the particles arrive at sea south of Sicily.

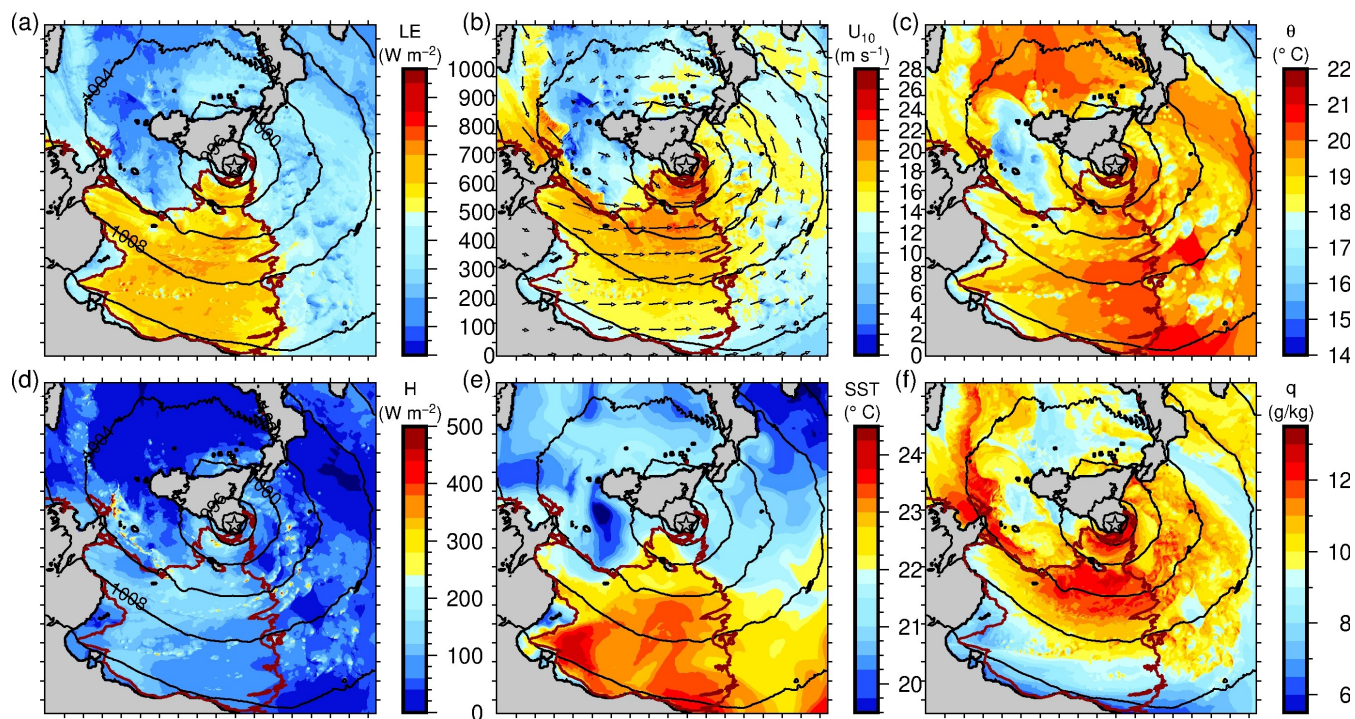


Figure 18: Same as Figure 13 but at 18:00 UTC on 7 November.

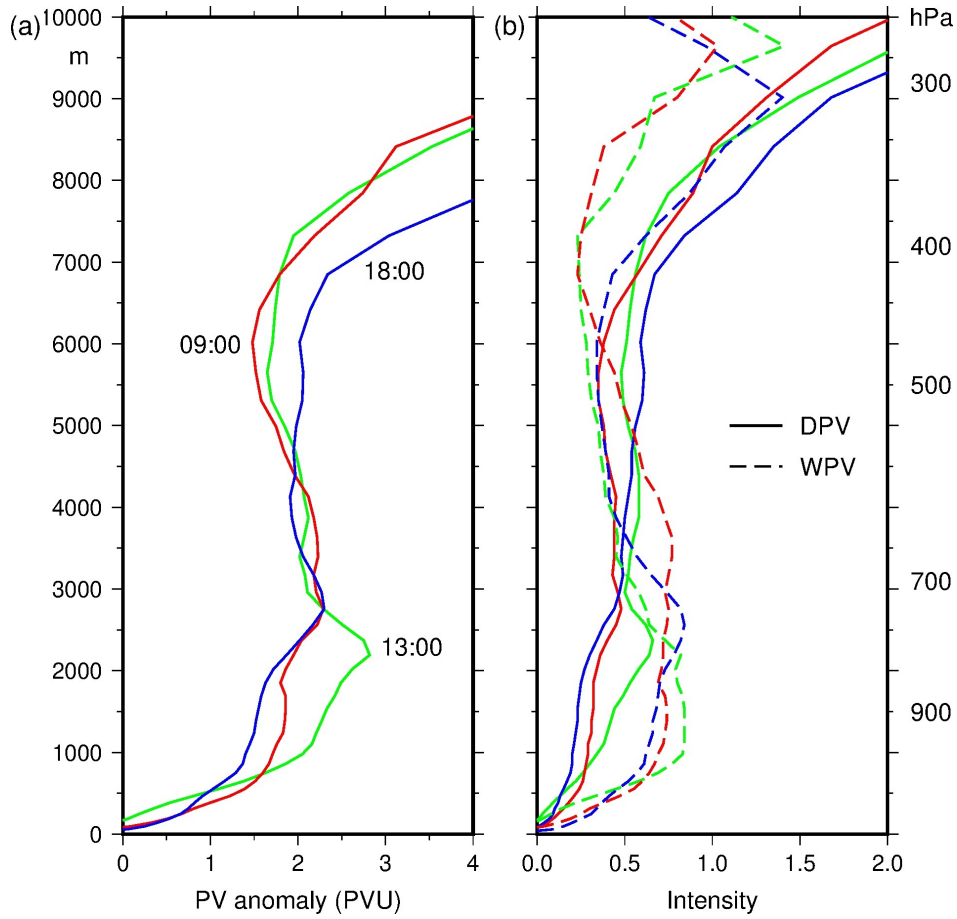


Figure 19: Vertical profiles of PV (a), and DPV and WPV (b) averaged within a 100-km radius circle around the cyclone centre at 09:00 (red), 13:00 (green) and 18:00 UTC (blue) on 7 November, in the CPL simulation.